



HAL
open science

Coherence of coupling conditions for the isothermal Euler system

Andrea Corli, Ulrich Razafison, Massimiliano D Rosini

► **To cite this version:**

Andrea Corli, Ulrich Razafison, Massimiliano D Rosini. Coherence of coupling conditions for the isothermal Euler system. 2024. hal-04480045

HAL Id: hal-04480045

<https://hal.science/hal-04480045>

Preprint submitted on 27 Feb 2024

HAL is a multi-disciplinary open access archive for the deposit and dissemination of scientific research documents, whether they are published or not. The documents may come from teaching and research institutions in France or abroad, or from public or private research centers.

L'archive ouverte pluridisciplinaire **HAL**, est destinée au dépôt et à la diffusion de documents scientifiques de niveau recherche, publiés ou non, émanant des établissements d'enseignement et de recherche français ou étrangers, des laboratoires publics ou privés.

Coherence of coupling conditions for the isothermal Euler system

Andrea Corli^a, Ulrich Razafison^b, Massimiliano D. Rosini^{c,d}

^a*Department of Mathematics and Computer Science, University of Ferrara
I-44121 Italy*

^b*Université de Franche-Comté, CNRS, UMR 6623, LmB
F-25000 Besançon, France*

^c*Uniwersytet Marii Curie-Skłodowskiej, Plac Marii Curie-Skłodowskiej 1
20-031 Lublin, Poland*

^d*Department of Management and Business Administration,
University “G. d’Annunzio of Chieti-Pescara”, viale Pindaro, 42, Pescara, 65127, Italy*

February 27, 2024

Abstract

We consider an isothermal flow through two pipes. At the junction, the flow is possibly modified by some devices, such as valves, compressors, and so on, or by the geometry of the junction; coupling conditions between the traces of the flow must be given. We first provide a general framework to model this situation by means of constrained Riemann problems, and provide some theoretical results. A key issue for both the validity of a coupling model and the robustness of numerical schemes to find solutions is whether the coupling Riemann solver is coherent. This property implies that applying the coupling Riemann solver to the traces at the junction of a coupling solution results in finding the same solution locally. We also give theoretical results for coherence. Then, we consider several couplings; we discuss the uniqueness of the corresponding solvers and, in particular, their coherence. Surprisingly, some solvers of wide use are proven not to be uniquely defined, and others are not coherent. We present numerical examples to illustrate this property.

1 Introduction

In this paper we study the mathematical properties of several modelings, in one space dimension, of gas flows through a *coupling* connecting two pipes. Couplings may arise in several ways: they can model the presence of either a compressor or a valve between the pipes, or they can simply model different characteristics of the pipes. Coupling conditions may regard the continuity of either the pressure or the dynamical pressure; they may impose an increase or a decrease of the pressure; they can maximize the flow, and so on. Moreover, the flow may be assumed to take place in a single direction (one-way flow) or in both directions (two-way flow). There are really many papers dealing with this subject, both from a mathematical and engineering point of view; we refer to the following sections for detailed references. We refer to [8] for a survey on flows in networks. Usually, coupling conditions are provided either on a phenomenological basis or to simulate the behavior of a device at the junction (a valve, a compressor and so on). We refer to [5,6] for the derivation of entropic coupling conditions for macroscopic models from kinetic ones in the case of Burgers or a linear wave equation, respectively, and to [42,43] for a general theory.

About the gas flow along the two pipes, for simplicity we focus on the isothermal case and the 2×2 Euler system in one space dimension; it is a strictly hyperbolic system of conservation laws. This allows us to point out some important mathematical aspects of the modelling of the coupling, which have been previously discarded, without dealing with heavy computations. More precisely, we analyze the Riemann solvers that encode a coupling placed at $x = 0$, briefly called *c-Riemann solvers*. In most cases, they differ from the Lax Riemann solver [45]. A common feature among most of them

is that, at $x = 0$, they satisfy the Rankine-Hugoniot condition for mass conservation, but not always that for the conservation of momentum.

This paper addresses three main issues.

- A first issue is whether a coupling condition singles out a *unique* c-Riemann solver; rather surprisingly, we shall show that this is not the case in many modelings.
- Once the previous problem has been settled, one can investigate the *coherence* of the c-Riemann solver, which means the following, roughly speaking. Consider some Riemann data and find the corresponding (self-similar) *c-solution* $u_1 = u_1(x/t)$; now, consider the two traces $u_1^- \doteq u_1(0^-)$ and $u_1^+ \doteq u_1(0^+)$ of the solution at $x = 0$, use them as Riemann data and find the corresponding c-solution $u_2 = u_2(x/t)$. If u_2 coincides with u_1^\pm in $\pm x > 0$, then the solver is *coherent*. This property, which is satisfied by the Lax Riemann solver, is fundamental both as a test for the validity of the model and for the robustness of the numerical schemes that one can use to find a c-solution. Similarly to the previous issue, we shall prove that coherence does not always hold. Coherence was investigated for several original models of gas flows through valves in [19–22]; in that case, the lack of coherence gives rise to the phenomenon of *chattering*. As far as numerics are concerned, incoherence leads to instabilities of the numerical schemes, resulting in the appearance of oscillations in the numerical simulations, see for instance Figures 15c and 15d.
- The third issue concerns *supersonic flows*. The assumption of subsonic flows is done in most papers on two bases: in applications, flows are often subsonic (but not always, see [35, 48] and references therein), and their mathematical treatment is simpler because the number of waves in a c-solution is less. However, the Lax Riemann solver for the isothermal Euler system can involve supersonic states even if both initial data are subsonic. So, we do not assume, in general, that flows are subsonic.

We do not propose any new models, but provide both a general framework to tackle the previous issues and a detailed analysis of several coupling models. As we mentioned above, we restrict ourselves to the isothermal Euler system for the gas flow; nevertheless, we study in that framework also some models originally proposed either for isentropic flows, or including viscosity or else friction terms due to the pipe walls. Indeed, about the two latter terms, their effect can be neglected when one focuses on the flow behavior at the junction. The long reference list shows our effort to encompass most of the relevant models occurring in the literature; papers dealing with the Euler 3×3 system or other models have been omitted for brevity.

Here follows an outline of the paper. Section 2 reviews some structural properties of the isothermal Euler system; we also provide several definitions to be used in the following. In Section 3 we introduce the c-Riemann solvers and prove a general result on coherence, namely, Theorem 3.8. Sections from 4 onward focus on applications. More precisely, Sections 4 and 5 deal with “free” flows, Section 6 investigates the case of compressors, Section 7 deals with valves, and Section 8 addresses resistors. In the last Section 9 we first summarize in Table 1 the results about uniqueness and coherence of the c-Riemann solvers we analyzed; then we draw some general conclusions and give some directions for future work on this subject.

The main results concern a detailed analysis of the continuity conditions (on pressure, dynamic pressure or specific enthalpy) in Section 4 for general two-way flows. Section 5 specializes this analysis to the case of one-way flows, allowing however possibly different pressure laws in the pipes. If flows are assumed to be subsonic or sonic, then Proposition 5.1 shows the coherence of the corresponding solver; on the contrary, if we require the continuity of the pressure and the maximization of the flow at $x = 0$, then Proposition 5.3 proves that the related solver is *not* coherent if the pressure laws differ. About compressors, Propositions 6.3 and 6.5 prove the coherence of two different solvers. About valves, we first comments on the (several) related results proved in [19–22]; then we show that other modelings proposed in the literature either do not lead to a unique solver or, when this happens, the solver is incoherent.

2 Euler equations: the flow along a tube

In this section we introduce the isothermal Euler equation and recall the properties of the Lax curves. The figures concerning Lax and related curves are obtained by a numerical software; so they are

“exact”. They are shown in the case $a = 1$, unless otherwise specified.

2.1 The system

The gas flow along a pipe is governed by the isothermal Euler equations

$$\begin{cases} \rho_t + q_x = 0, \\ q_t + P_x = 0, \end{cases} \quad (2.1)$$

where $\rho = \rho(t, x)$ is the *density*, $q = q(t, x)$ the *momentum* at time $t \geq 0$ and position $x \in \mathbb{R}$, and

$$P(\rho, q) \doteq \frac{q^2}{\rho} + p(\rho) \quad (2.2)$$

the *flow of the momentum* or *dynamic pressure*. Above, we denoted by

$$p(\rho) = a^2 \rho \quad (2.3)$$

the *pressure* and the constant $a > 0$ is the *sound speed*. We also define the *velocity*

$$v(\rho, q) \doteq q/\rho.$$

A state $u \doteq (\rho, q)$ is *subsonic* if $|v(u)| < a$, *sonic* if $|v(u)| = a$ and *supersonic* if $|v(u)| > a$. We recall that $|v(u)|/a$ is the *Mach number*. The graphs of the functions $s_{\pm}(\rho) \doteq \pm a \rho$ in the (ρ, q) -plane are the *sonic curves*. The eigenvalues of the Jacobian matrix of the flux $f(\rho, q) \doteq (q, P(\rho, q))^T$ of (2.1) are $\lambda_1(u) \doteq v(u) - a$ and $\lambda_2(u) \doteq v(u) + a$. System (2.1) is strictly hyperbolic in $\Omega \doteq \{(\rho, q) \in \mathbb{R}^2 : \rho > 0\}$ because $\lambda_1(u) < \lambda_2(u)$ for $u \in \Omega$. Both characteristic fields are genuinely nonlinear.

2.2 The Lax curves

For fixed $u_o \doteq (\rho_o, q_o) \in \Omega$ and $i \in \{1, 2\}$, we define the functions $\mathcal{FL}_i^{u_o}, \mathcal{BL}_i^{u_o} : (0, \infty) \rightarrow \mathbb{R}$ as

$$\begin{aligned} \mathcal{FL}_1^{u_o}(\rho) &\doteq \begin{cases} \mathcal{R}_1^{u_o}(\rho) & \text{if } \rho \in (0, \rho_o], \\ \mathcal{S}_1^{u_o}(\rho) & \text{if } \rho \in (\rho_o, \infty), \end{cases} & \mathcal{FL}_2^{u_o}(\rho) &\doteq \begin{cases} \mathcal{S}_2^{u_o}(\rho) & \text{if } \rho \in (0, \rho_o), \\ \mathcal{R}_2^{u_o}(\rho) & \text{if } \rho \in [\rho_o, \infty), \end{cases} \\ \mathcal{BL}_1^{u_o}(\rho) &\doteq \begin{cases} \mathcal{S}_1^{u_o}(\rho) & \text{if } \rho \in (0, \rho_o), \\ \mathcal{R}_1^{u_o}(\rho) & \text{if } \rho \in [\rho_o, \infty), \end{cases} & \mathcal{BL}_2^{u_o}(\rho) &\doteq \begin{cases} \mathcal{R}_2^{u_o}(\rho) & \text{if } \rho \in (0, \rho_o], \\ \mathcal{S}_2^{u_o}(\rho) & \text{if } \rho \in (\rho_o, \infty), \end{cases} \end{aligned}$$

with

$$\mathcal{R}_i^{u_o}(\rho) \doteq \left(\frac{q_o}{\rho_o} + (-1)^i a \ln \left(\frac{\rho}{\rho_o} \right) \right) \rho, \quad \mathcal{S}_i^{u_o}(\rho) \doteq \left(\frac{q_o}{\rho_o} + (-1)^i a \left(\sqrt{\frac{\rho}{\rho_o}} - \sqrt{\frac{\rho_o}{\rho}} \right) \right) \rho.$$

The graphs of the functions $\mathcal{FL}_i^{u_o}$ and $\mathcal{BL}_i^{u_o}$ are the *forward FL* $_i^{u_o}$ and *backward BL* $_i^{u_o}$ *Lax curves* of the i -th family through u_o , see Figure 1. Analogously, the *shock S* $_i^{u_o}$ and *rarefaction R* $_i^{u_o}$ *curves* through u_o are the graphs of the functions $\mathcal{S}_i^{u_o}$ and $\mathcal{R}_i^{u_o}$. The i -shock speed between (ρ_o, q_o) and (ρ, q) is $s_i^{u_o}(\rho) \doteq v(\rho_o, q_o) + (-1)^i a \sqrt{\rho/\rho_o}$.

In the following lemma we collect the main properties of the above functions, see [19, Proposition 2.4].

Lemma 2.1. *Let $u_o \doteq (\rho_o, q_o), u^o \doteq (\rho^o, q^o) \in \Omega$ be two distinct states and $i \in \{1, 2\}$. Then we have:*

- (a) $\mathcal{R}_1^{(\rho_o, -q_o)} \equiv -\mathcal{R}_2^{(\rho_o, q_o)}$ and $\mathcal{S}_1^{(\rho_o, -q_o)} \equiv -\mathcal{S}_2^{(\rho_o, q_o)}$.
- (b) $\mathcal{R}_i^{u_o}, \mathcal{S}_i^{u_o}, \mathcal{FL}_i^{u_o}$ and $\mathcal{BL}_i^{u_o}$ are \mathbf{C}^2 functions in $(0, \infty)$; moreover

$$\begin{aligned} \mathcal{R}_i^{u_o}(0^+) &= \mathcal{S}_i^{u_o}(0^+) = 0, & \frac{d\mathcal{R}_i^{u_o}}{d\rho}(0^+) &= \frac{d\mathcal{S}_i^{u_o}}{d\rho}(0^+) = (-1)^{i+1} \cdot \infty, \\ \mathcal{R}_i^{u_o}(\infty) &= \mathcal{S}_i^{u_o}(\infty) = (-1)^i \cdot \infty, & \frac{d\mathcal{R}_i^{u_o}}{d\rho}(\rho_o) &= \frac{d\mathcal{S}_i^{u_o}}{d\rho}(\rho_o) = \lambda_i(u_o). \end{aligned}$$

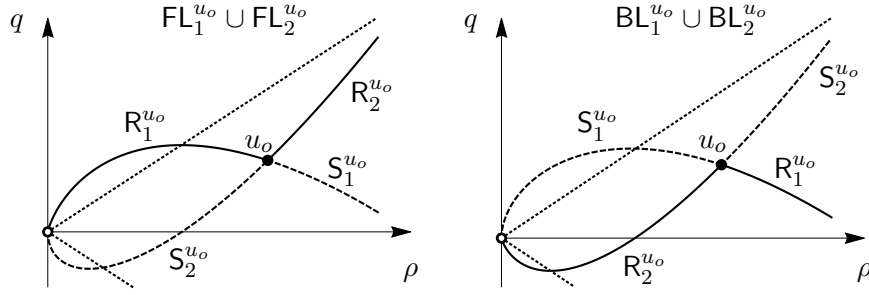


Figure 1: Forward and backward Lax curves through u_o . The solid lines refer to rarefaction curves $\mathcal{R}_i^{u_o}$, the dashed lines to shock curves $\mathcal{S}_i^{u_o}$, $i \in \{1, 2\}$, and the dotted lines to the sonic curves.

- (c) $\mathcal{R}_1^{u_o}, \mathcal{S}_1^{u_o}, \mathcal{FL}_1^{u_o}, \mathcal{BL}_1^{u_o}$ are strictly concave, while $\mathcal{R}_2^{u_o}, \mathcal{S}_2^{u_o}, \mathcal{FL}_2^{u_o}, \mathcal{BL}_2^{u_o}$ are strictly convex.
- (d) $\mathcal{S}_2^{u_o}(\rho) = \mathcal{FL}_2^{u_o}(\rho) < \mathcal{R}_2^{u_o}(\rho) = \mathcal{BL}_2^{u_o}(\rho) < \mathcal{R}_1^{u_o}(\rho) = \mathcal{FL}_1^{u_o}(\rho) < \mathcal{S}_1^{u_o}(\rho) = \mathcal{BL}_1^{u_o}(\rho)$ in $(0, \rho_o)$ and $\mathcal{S}_1^{u_o}(\rho) = \mathcal{FL}_1^{u_o}(\rho) < \mathcal{R}_1^{u_o}(\rho) = \mathcal{BL}_1^{u_o}(\rho) < \mathcal{R}_2^{u_o}(\rho) = \mathcal{FL}_2^{u_o}(\rho) < \mathcal{S}_2^{u_o}(\rho) = \mathcal{BL}_2^{u_o}(\rho)$ in (ρ_o, ∞) .
- (e) $u_o \in \mathcal{R}_i^{u_o} \cap \mathcal{S}_i^{u_o} \cap \mathcal{FL}_i^{u_o} \cap \mathcal{BL}_i^{u_o}$.
- (f) $\mathcal{R}_i^{u_o} \cap \mathcal{R}_i^{u^o} \neq \emptyset$ if and only if $\mathcal{R}_i^{u^o} = \mathcal{R}_i^{u_o}$, while if $u^o \in \mathcal{S}_i^{u_o}$ then $\mathcal{S}_i^{u_o} \cap \mathcal{S}_i^{u^o} = \{u_o, u^o\}$.

The following lemma shows that along a Lax curve of the first (respectively, second) family the velocity v is a decreasing (respectively, increasing) function of the density ρ , see [21, Lemma 2.4].

Lemma 2.2. Consider two states $u_1 \neq u_2$ in Ω , and either $u_1, u_2 \in \mathcal{FL}_i^{u_o}$ or $u_1, u_2 \in \mathcal{BL}_i^{u_o}$ for $i \in \{1, 2\}$. Then

$$(-1)^i (\rho_1 - \rho_2) (v(u_1) - v(u_2)) > 0.$$

We now introduce some notation; we refer to Figure 2.

Definition 2.3. For $u_\ell, u_r \in \Omega$ we define:

- $\bar{u}(u_\ell) \doteq (\bar{\rho}(u_\ell), \bar{q}(u_\ell))$ is the element of $\mathcal{FL}_1^{u_\ell}$ with the maximum q -coordinate;
- $\underline{u}(u_r) \doteq (\underline{\rho}(u_r), \underline{q}(u_r))$ is the element of $\mathcal{BL}_2^{u_r}$ with the minimum q -coordinate;
- $\tilde{u}(u_\ell, u_r) \doteq (\tilde{\rho}(u_\ell, u_r), \tilde{q}(u_\ell, u_r))$ is the (unique) element of $\mathcal{FL}_1^{u_\ell} \cap \mathcal{BL}_2^{u_r}$;
- for $q_o \leq \bar{q}(u_\ell)$, let $\hat{u}(q_o, u_\ell) \doteq (\hat{\rho}(q_o, u_\ell), q_o)$ be the intersection of $\mathcal{FL}_1^{u_\ell}$ and $q = q_o$ with the largest ρ -coordinate;
- for $q_o \geq \underline{q}(u_r)$, let $\check{u}(q_o, u_r) \doteq (\check{\rho}(q_o, u_r), q_o)$ be the intersection of $\mathcal{BL}_2^{u_r}$ and $q = q_o$ with the largest ρ -coordinate;
- let $u_a(u_\ell) \doteq (\rho_a(u_\ell), q_a(u_\ell))$ be the (unique) intersection of $\mathcal{FL}_1^{u_\ell}$ with the sonic line $q = -a\rho$ in Ω ;
- let $u^a(u_r) \doteq (\rho^a(u_r), q^a(u_r))$ be the (unique) intersection of $\mathcal{BL}_2^{u_r}$ with the sonic line $q = a\rho$ in Ω .

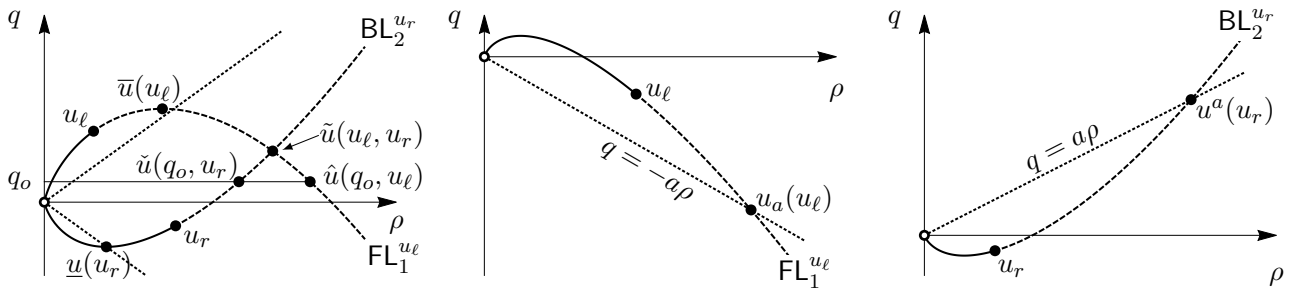


Figure 2: Notation in Definition 2.3. Rarefaction, shock and sonic curves are depicted as in Figure 1.

Observe that $\hat{\rho}(q_o, u_\ell) \geq \bar{\rho}(u_\ell)$, $\check{\rho}(q_o, u_r) \geq \underline{\rho}(u_r)$ and $\hat{q}(q_o, u_\ell) = q_o = \check{q}(q_o, u_r)$ if $\hat{u}(q_o, u_\ell)$ and $\check{u}(q_o, u_r)$ are well defined, see Figure 2. Moreover, by (b) and (c) in Lemma 2.1, we have $\bar{\rho}(u_\ell), \underline{\rho}(u_r) > 0$ as well as $\bar{q}(u_\ell) > 0 > \underline{q}(u_r)$.

In the following proposition we show that if the maximum of $\rho \mapsto \mathcal{FL}_1^{u_\ell}(\rho)$ is attained on the left of ρ_ℓ , then it is a sonic state, otherwise it is a supersonic state. Analogously, if the minimum of $\rho \mapsto \mathcal{BL}_2^{u_r}(\rho)$ is attained on the left of ρ_r , then it is a sonic state, otherwise it is a supersonic state.

Proposition 2.4.

- (a) If $\bar{\rho}(u_\ell) \leq \rho_\ell$, then $v(\bar{u}(u_\ell)) = a$.
- (b) If $\bar{\rho}(u_\ell) > \rho_\ell$, then $v(\bar{u}(u_\ell)) > a$.
- (c) If $\underline{\rho}(u_r) \leq \rho_r$, then $v(\underline{u}(u_r)) = -a$.
- (d) If $\underline{\rho}(u_r) > \rho_r$, then $v(\underline{u}(u_r)) < -a$.

We defer to [21, § 7.1] for the proof. For later use, we also provide the following result.

Proposition 2.5. *If $v(u_\ell) > a$ then $0 < v(\hat{u}(q_\ell, u_\ell)) < a$. Analogously, if $v(u_r) < -a$ then $-a < v(\tilde{u}(q_r, u_r)) < 0$.*

Proof. We only prove the former statement. For simplicity, we denote $\hat{u} = \hat{u}(q_\ell, u_\ell)$. Clearly $q_\ell > 0$ implies $v(\hat{u}) > 0$. By hypothesis we have $v(u_\ell) > a$; hence, by (b) and (c) in Lemma 2.1 and the definition of \bar{u} in Definition 2.3, we deduce $\rho_\ell < \bar{\rho}(u_\ell) < \hat{\rho}$ and, consequently, $\hat{u} \in \mathcal{S}_1^{u_\ell}$. Moreover, by definition we have $\hat{q} = q_\ell$, and hence

$$\frac{q_\ell}{\hat{\rho}} = v(\hat{u}) = \frac{1}{\hat{\rho}} \mathcal{S}_1^{u_\ell}(\hat{\rho}) = \frac{q_\ell}{\rho_\ell} - a \left(\sqrt{\frac{\hat{\rho}}{\rho_\ell}} - \sqrt{\frac{\rho_\ell}{\hat{\rho}}} \right).$$

The above condition is equivalent to $q_\ell(1/\rho_\ell - 1/\hat{\rho}) = a(\hat{\rho} - \rho_\ell)/(\sqrt{\rho_\ell \hat{\rho}})$ which, in turn, is equivalent to $q_\ell = a\sqrt{\rho_\ell \hat{\rho}}$, and therefore $v(\hat{u}) = q_\ell/\hat{\rho} = a\sqrt{\rho_\ell/\hat{\rho}} < a$. \square

2.3 The Riemann problem

For any pair of constant states $u_\ell, u_r \in \Omega$, the Riemann problem for system (2.1) is the initial-value problem with initial condition

$$u(0, x) = \begin{cases} u_\ell & \text{if } x < 0, \\ u_r & \text{if } x \geq 0. \end{cases} \quad (2.4)$$

Definition 2.6. *A function $u = (\rho, q) \in \mathbf{C}^0([0, \infty); \mathbf{BV}(\mathbb{R}; \Omega))$ is a weak solution of Riemann problem (2.1), (2.4) in $[0, \infty) \times \mathbb{R}$ if for any test function $\varphi \in \mathbf{C}_c^\infty([0, \infty) \times \mathbb{R}; \mathbb{R})$ we have*

$$\begin{aligned} \int_0^\infty \int_{\mathbb{R}} [\rho \varphi_t + q \varphi_x] dx dt + \rho_\ell \int_{-\infty}^0 \varphi(0, x) dx + \rho_r \int_0^\infty \varphi(0, x) dx &= 0, \\ \int_0^\infty \int_{\mathbb{R}} [q \varphi_t + P(\rho, q) \varphi_x] dx dt + q_\ell \int_{-\infty}^0 \varphi(0, x) dx + q_r \int_0^\infty \varphi(0, x) dx &= 0. \end{aligned}$$

Any smooth discontinuity curve $x = \gamma(t)$ of a piecewise regular weak solution $u = (\rho, q)$ of (2.1) satisfies the Rankine-Hugoniot conditions

$$(\rho^+ - \rho^-) \dot{\gamma} = q^+ - q^-, \quad (2.5)$$

$$(q^+ - q^-) \dot{\gamma} = P(\rho^+, q^+) - P(\rho^-, q^-), \quad (2.6)$$

where $u^\pm(t) \doteq u(t, \gamma(t)^\pm)$ are the traces of u along the discontinuity. Condition (2.5) ensures the conservation of the mass, while (2.6) encodes the conservation of momentum.

Define $\mathbf{D} \doteq \Omega \times \Omega$. We denote the standard Riemann solver of (2.1) by $\mathcal{RS}_p: \mathbf{D} \rightarrow \mathbf{BV}(\mathbb{R}; \Omega)$, see [45], and denote

$$u_p \doteq (\rho_p, q_p) \doteq \mathcal{RS}_p[u_\ell, u_r], \quad u_p^\pm \doteq (\rho_p^\pm, q_p^\pm) \doteq u_p(0^\pm). \quad (2.7)$$

The function $(t, x) \mapsto u_p(x/t)$ is a weak solution of the Riemann problem (2.1), (2.4) in $[0, \infty) \times \mathbb{R}$. Furthermore, $\xi \mapsto u_p(\xi)$ is chosen to be right continuous. Recall that if $u_\ell \neq \tilde{u}(u_\ell, u_r) \neq u_r$, then $\mathcal{RS}_p[u_\ell, u_r]$ is given by the juxtaposition of the 1-wave $\mathcal{RS}_p[u_\ell, \tilde{u}(u_\ell, u_r)]$ and the 2-wave

$\mathcal{RS}_p[\tilde{u}(u_\ell, u_r), u_r]$, where $\tilde{u}(u_\ell, u_r) \in \text{FL}_1^{u_\ell} \cap \text{BL}_2^{u_r}$ is given in Definition 2.3. We also recall that \mathcal{RS}_p is consistent [19, Proposition 2.5]; this means that, for any $(u_\ell, u_r) \in \text{D}$ and for any $\xi_0 \in \mathbb{R}$ we have $(u_\ell, u_p(\xi_0)), (u_p(\xi_0), u_r) \in \text{D}$, as well as both

$$\begin{aligned} \mathcal{RS}_p[u_\ell, u_p(\xi_0)](\xi) &= \begin{cases} u_p(\xi) & \text{if } \xi < \xi_0, \\ u_p(\xi_0) & \text{if } \xi \geq \xi_0, \end{cases} & \text{and} & u_p(\xi) = \begin{cases} \mathcal{RS}_p[u_\ell, u_p(\xi_0)] & \text{if } \xi < \xi_0, \\ \mathcal{RS}_p[u_p(\xi_0), u_r] & \text{if } \xi \geq \xi_0. \end{cases} \\ \mathcal{RS}_p[u_p(\xi_0), u_r](\xi) &= \begin{cases} u_p(\xi_0) & \text{if } \xi < \xi_0, \\ u_p(\xi) & \text{if } \xi \geq \xi_0, \end{cases} \end{aligned}$$

2.3.1 Properties of the speed of the waves

We now search for conditions in order that u_p has a 2-wave with non-positive speed, as well as conditions in order that u_p has a 1-wave with non-negative speed; this issue plays an important role in the following. We refer to Figure 3.

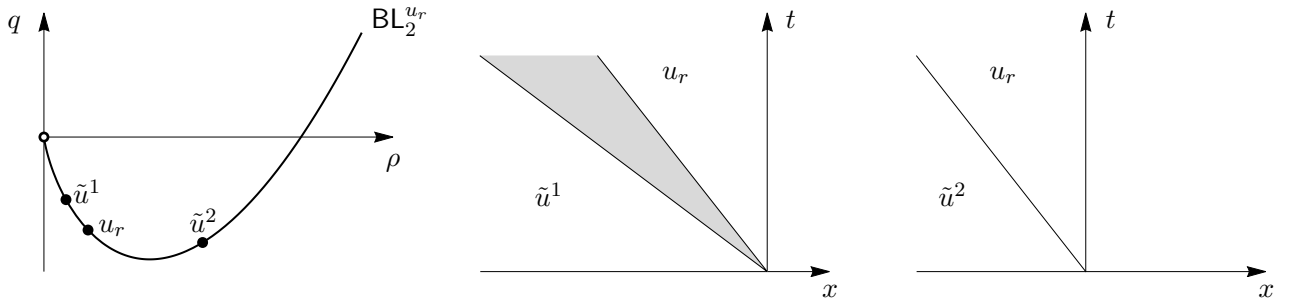


Figure 3: 2-waves $\mathcal{RS}_p[\tilde{u}, u_r]$ with negative speed. Above, \tilde{u}^i , $i \in \{1, 2\}$, are two possible choices for $\tilde{u}(u_\ell, u_r)$; here \tilde{u}^1 corresponds to a 2-rarefaction and \tilde{u}^2 to a 2-shock.

Proposition 2.7. *We have the following.*

(a) $\mathcal{RS}_p[u_\ell, u_r]$ has a 2-wave with non-positive speed and $\mathcal{RS}_p[u_\ell, u_r](0^-) = u_r$ if and only if

$$\rho_r \leq \underline{\rho}(u_r), \quad (\tilde{\rho}(u_\ell, u_r) - \rho_r)(\tilde{q}(u_\ell, u_r) - q_r) < 0. \quad (2.8)$$

In particular, (2.8) implies $v(u_r) \leq -a$, $q_r < 0$ and $\tilde{q}(u_\ell, u_r) < 0$.

(b) $\mathcal{RS}_p[u_\ell, u_r]$ has a 1-wave with non-negative speed and $\mathcal{RS}_p[u_\ell, u_r](0^+) = u_\ell$ if and only if

$$\rho_\ell \leq \bar{\rho}(u_\ell), \quad (\tilde{\rho}(u_\ell, u_r) - \rho_\ell)(\tilde{q}(u_\ell, u_r) - q_\ell) > 0. \quad (2.9)$$

In particular, (2.9) implies $v(u_\ell) \geq a$, $q_\ell > 0$ and $\tilde{q}(u_\ell, u_r) > 0$.

Proof. We only show the first statement; the proof of the second one is analogous.

The Riemann solver $\mathcal{RS}_p[u_\ell, u_r]$ has at most two waves by its very definition. If this is the case, then the first is the 1-wave $\mathcal{RS}_p[u_\ell, \tilde{u}]$ and the second is the 2-wave $\mathcal{RS}_p[\tilde{u}, u_r]$, where $\tilde{u} \doteq (\tilde{\rho}, \tilde{q}) \doteq \tilde{u}(u_\ell, u_r)$.

The 2-wave has non-positive speed and $\mathcal{RS}_p[u_\ell, u_r](0^-) = u_r$ if and only if either it is a 2-shock with $\rho_r < \min\{\tilde{\rho}, \underline{\rho}(u_r)\}$ and $\tilde{q} < q_r < 0$, or it is a 2-rarefaction with $\tilde{\rho} < \rho_r \leq \underline{\rho}(u_r)$ and $q_r < \tilde{q} < 0$, see Figure 3. It is now clear that one of the two cases occurs if and only if (2.8) is satisfied.

We prove the last statement. If $\rho_r = \underline{\rho}(u_r)$, then $u_r = \underline{u}(u_r)$ and $v(u_r) = -a$ by (c) in Proposition 2.4. If $\rho_r < \underline{\rho}(u_r)$, then $v(u_r) < -a$ by (d) in Proposition 2.4 and Lemma 2.2 with $i = 2$. \square

We now generalize the results of Proposition 2.7. More precisely, in Proposition 2.8 we fix u_ℓ and describe the states u_r such that (2.10) holds true; in Proposition 2.9 we fix u_r and describe the states u_ℓ such that (2.11) holds true. Notice that (2.8) implies (2.10), while (2.9) implies (2.11). Furthermore, formula (2.10) implies $\mathcal{RS}_p[u_\ell, u_r](0) = u_r$ by construction of \mathcal{RS}_p ; hence, we have $\mathcal{RS}_p[u_\ell, u_r](\xi) = u_r$ for any $\xi \geq 0$, since \mathcal{RS}_p is consistent, and therefore $\mathcal{RS}_p[u_\ell, u_r]$ has neither

waves with positive speed nor a stationary shock. Analogously, (2.11) implies that $\mathcal{RS}_p[u_\ell, u_r]$ has neither waves with negative speed nor a stationary shock. Given the symmetry inherent in the problem, we prove only Proposition 2.9.

Proposition 2.8. Fix $u_\ell \in \Omega$ and consider $u_a = u_a(u_\ell)$. A state $u_r \in \Omega$ is such that

$$\mathcal{RS}_p[u_\ell, u_r](0^-) = u_r \quad (2.10)$$

if and only if one of the following conditions holds true:

- (I) $u_r \in \text{FL}_1^{u_\ell}$ and either $v(u_\ell) > a$ and $\rho_r \in \{\rho_\ell\} \cup (\hat{\rho}(q_\ell, u_\ell), \infty)$, or $v(u_\ell) \leq a$ and $\rho_r \geq \bar{\rho}(u_\ell)$;
- (II) $q_r \leq \mathcal{FL}_2^{u_a}(\rho_r)$ and $v(u_r) \leq -a$,
- (III) $0 > q_r > \tilde{q}(u_\ell, u_r) > q_a$ and $\rho_r < \underline{\rho}(u_r)$.

In particular, in case (I) $\mathcal{RS}_p[u_\ell, u_r]$ consists of a one wave (a 1-wave) at most; when (II) or (III) are satisfied but not (I), then $\mathcal{RS}_p[u_\ell, u_r]$ consists of two waves (a 1-wave and a 2-wave) at most. Moreover, if u_r is subsonic, i.e., $|v(u_r)| < a$, then it satisfies (I) and $\rho_r < \rho_a$.

Proposition 2.9. Fix $u_r \in \Omega$ and consider $u^a = u^a(u_r)$. A state $u_\ell \in \Omega$ is such that

$$\mathcal{RS}_p[u_\ell, u_r](0^+) = u_\ell \quad (2.11)$$

if and only if one of the following conditions holds true:

- (I) $u_\ell \in \text{BL}_2^{u_r}$ and either $v(u_r) < -a$ and $\rho_\ell \in \{\rho_r\} \cup (\check{\rho}(q_r, u_r), \infty)$, or $v(u_r) \geq -a$ and $\rho_\ell \geq \underline{\rho}(u_r)$,
- (II) $q_\ell \geq \mathcal{BL}_1^{u^a}(\rho_\ell)$ and $v(u_\ell) \geq a$,
- (III) $0 < q_\ell < \tilde{q}(u_\ell, u_r) < q^a$ and $\rho_\ell < \bar{\rho}(u_\ell)$.

In particular, in case (I) $\mathcal{RS}_p[u_\ell, u_r]$ consists of a one wave (a 2-wave) at most; when (II) or (III) are satisfied but not (I), then $\mathcal{RS}_p[u_\ell, u_r]$ consists of two waves (a 1-wave and a 2-wave) at most. Moreover, if u_ℓ is subsonic, i.e., $|v(u_\ell)| < a$, then it satisfies (I) and $\rho_\ell < \rho^a$.

Proof of Proposition 2.9. Assume that u_ℓ satisfies (I). We distinguish the following cases. If $u_\ell = u_r$, then $\mathcal{RS}_p[u_\ell, u_r] \equiv u_\ell$. If $u_\ell \in \text{BL}_2^{u_r}$, $v(u_r) < -a$ and $\rho_\ell \in (\check{\rho}(q_r, u_r), \infty)$, then $\mathcal{RS}_p[u_\ell, u_r]$ has only a 2-shock with strictly positive speed. If $u_\ell \in \text{BL}_2^{u_r}$, $v(u_r) \geq -a$ and $\rho_\ell \in [\underline{\rho}(u_r), \infty) \setminus \{u_r\}$, then $\mathcal{RS}_p[u_\ell, u_r]$ has only a 2-shock with strictly positive speed if $\rho_\ell > \rho_r$ and a 2-rarefaction with positive speed if $\rho_\ell < \rho_r$. In any of these cases (2.11) follows.

Assume that u_ℓ satisfies (II) but not (I). If u_ℓ lies on the left of $\text{BL}_2^{u_r}$, then $\mathcal{RS}_p[u_\ell, u_r]$ has a 1-shock with strictly positive speed and, if $\tilde{u}(u_\ell, u_r) \neq u_r$, it also has a 2-wave with strictly positive speed. If u_ℓ lies on the right of $\text{BL}_2^{u_r}$, then $\mathcal{RS}_p[u_\ell, u_r]$ has a 1-rarefaction with positive speed and, if $\tilde{u}(u_\ell, u_r) \neq u_r$, it also has a 2-wave with strictly positive speed. In both cases (2.11) follows.

Assume that u_ℓ satisfies (III). In this case $\mathcal{RS}_p[u_\ell, u_r]$ has a 1-shock with strictly positive speed and, if $\tilde{u}(u_\ell, u_r) \neq u_r$, it also has a 2-wave with strictly positive speed; again (2.11) follows.

Conversely, it is then easy to prove that (I)-(III) describe the only possible cases to have (2.11).

We now prove the last statement. If u_ℓ is subsonic, then by (b) in Proposition 2.7 and the fact that $\mathcal{RS}_p[u_\ell, u_r]$ has only waves with non-negative speed it follows that $\mathcal{RS}_p[u_\ell, u_r]$ has no 1-waves, and then $u_\ell \in \text{BL}_2^{u_r}$. Moreover $\rho_\ell \geq \check{\rho}(0, u_r)$ because $q_\ell \geq 0$, and $\rho_\ell < \rho^a$ because u_ℓ is subsonic. \square

For any $u_\ell, u_r \in \Omega$, we denote, see Figures 4 and 5,

$$\Gamma^-(u_\ell) \doteq \{u_r \in \Omega : u_r \text{ satisfies one of conditions (I)-(III) in Proposition 2.8}\}, \quad (2.12)$$

$$\Gamma^+(u_r) \doteq \{u_\ell \in \Omega : u_\ell \text{ satisfies one of conditions (I)-(III) in Proposition 2.9}\}. \quad (2.13)$$

Notice that the isentropic counterpart of Figure 5 is represented in [29, Figure 10], of Figure 4 in [26, Figure 2.7] and when $q_\ell = 0$ in [43, Figure 3]. This shows that our approach (at least for the isothermal case) is sufficiently general to encompass several different cases. We denote by $B^-(u_\ell)$ the upper boundary of the set identified by (III) in Proposition 2.8; analogously, we denote by $B^+(u_r)$ the lower boundary of the set characterized by (III) in Proposition 2.9.

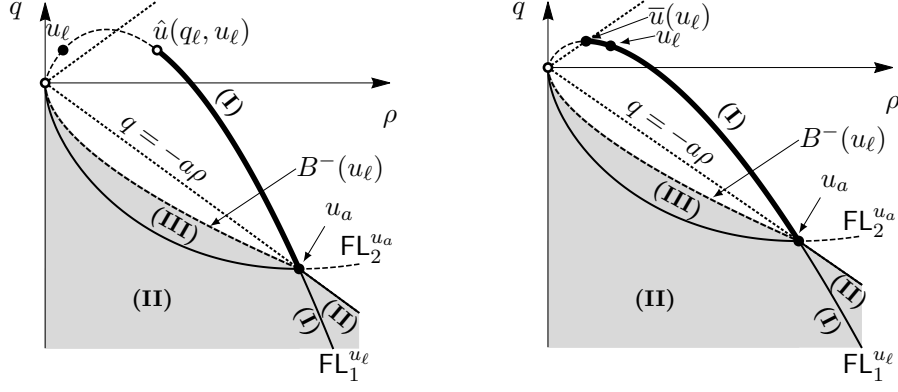


Figure 4: The set $\Gamma^-(u_\ell)$ (shaded regions, solid lines and the full points, but not the dashed lines) in (2.12). On the left the case $v(u_\ell) > a$, on the right the case $v(u_\ell) < a$.

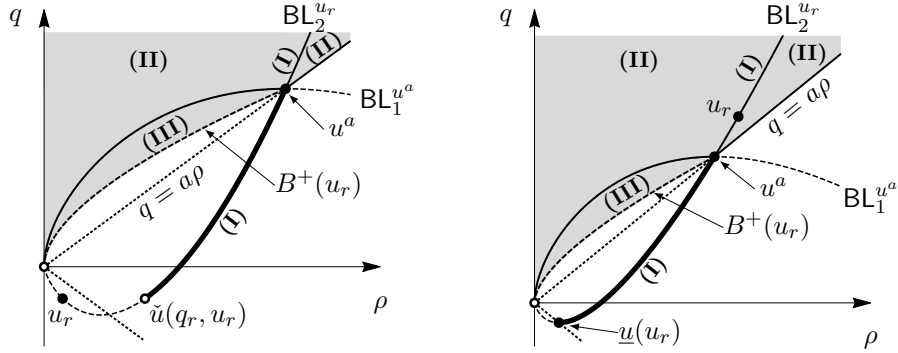


Figure 5: The set $\Gamma^+(u_r)$ (shaded regions, solid lines and the full points, but not the dashed lines) in (2.13). On the left the case $v(u_r) < -a$, on the right the case $v(u_r) > -a$.

2.3.2 Properties of the speed of the waves in the one-way case

In Corollaries 2.10 and 2.11 we study some properties of u_p analogous to those considered in Propositions 2.8 and 2.9, respectively, but in the case of a *one-way* flow, i.e., $q_p \geq 0$.

Corollary 2.10. *Fix $u_\ell \in \Omega$ with $q_\ell \geq 0$. A state $u_r \in \Omega$ is such that*

- (i) $\mathcal{RS}_p[u_\ell, u_r](0^-) = u_r$,
- (ii) $v(\mathcal{RS}_p[u_\ell, u_r]) \geq 0$,

if and only if $u_r \in \text{FL}_1^{u_\ell}$ and one of the following conditions holds true:

- (I) u_ℓ is supersonic and either $u_r = u_\ell$ or $\rho_r \in (\hat{\rho}(q_\ell, u_\ell), \hat{\rho}(0, u_\ell)]$,
- (II) u_ℓ is non-supersonic and $\rho_r \in [\bar{\rho}(u_\ell), \hat{\rho}(0, u_\ell)]$.

In particular, in all the above cases, $\mathcal{RS}_p[u_\ell, u_r]$ consists of a one wave (a 1-wave) at most.

Moreover, if u_r is supersonic, i.e., $v(u_r) > a$, then also u_ℓ is supersonic and $u_r = u_\ell$, see the picture on the left in Figure 6.

Proof. By Proposition 2.7, items (i) and (ii) imply that $\mathcal{RS}_p[u_\ell, u_r]$ doesn't have a 2-wave and then $u_r \in \text{FL}_1^{u_\ell}$. It is now clear by (i) that either (I) or (II) holds true, see Figure 6. More precisely, in case (I) $\mathcal{RS}_p[u_\ell, u_r]$ is either constant or a 1-shock, while in case (II) $\mathcal{RS}_p[u_\ell, u_r]$ is a 1-rarefaction if $\rho_r \in [\bar{\rho}(u_\ell), \rho_\ell)$, a constant if $\rho_r = \rho_\ell$ and a 1-shock if $\rho_r \in (\rho_\ell, \hat{\rho}(0, u_\ell)]$. The converse implication is obvious. The last statement easily follows from Proposition 2.5 and the above considerations. \square

For $u_\ell \in \Omega$ with $q_\ell \geq 0$, we denote

$$\Gamma_o^-(u_\ell) \doteq \{u_r \in \text{FL}_1^{u_\ell} : u_r \text{ satisfies (I) or (II) in Corollary 2.10}\}, \quad (2.14)$$

where “o” stands for one-way.

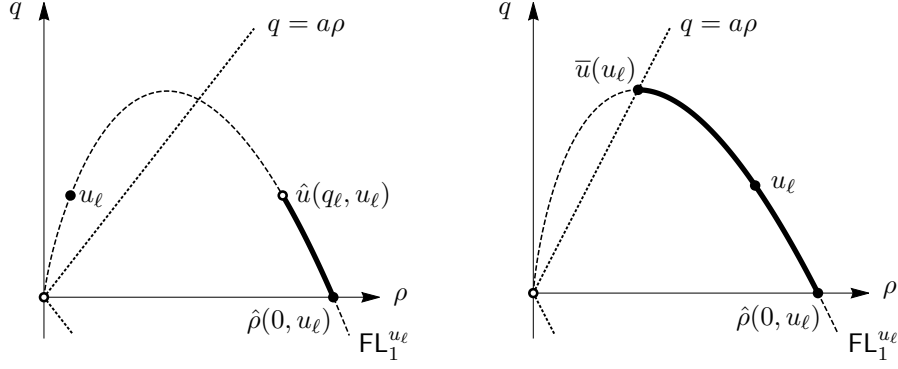


Figure 6: The set $\Gamma_o^-(u_\ell)$ (solid lines and the full points) in (2.14). On the left, case **(I)** in Corollary 2.10; on the right, case **(II)** in Corollary 2.10. The state $\hat{u}(q_\ell, u_\ell)$ on the left does not belong to the solid line.

Corollary 2.11. Fix $u_r \in \Omega$ with $q_r \geq 0$ and consider $u^a = u^a(u_r)$. A state $u_\ell \in \Omega$ is such that

- (i) $\mathcal{RS}_p[u_\ell, u_r](0^+) = u_\ell$,
- (ii) $v(\mathcal{RS}_p[u_\ell, u_r]) \geq 0$,

if and only if one of the following conditions holds true:

- (I)** $u_\ell \in \text{BL}_2^{u_r}$ and $q_\ell \geq 0$,
- (II)** $q_\ell \geq \mathcal{BL}_1^a(\rho_\ell)$ and $v(u_\ell) \geq a$,
- (III)** $0 < q_\ell < \tilde{q}(u_\ell, u_r) < q^a$ and $\rho_\ell < \bar{\rho}(u_\ell)$.

In particular, in case **(I)** $\mathcal{RS}_p[u_\ell, u_r]$ consists of a one wave (a 2-wave) at most; when **(II)** or **(III)** are satisfied but not **(I)**, then $\mathcal{RS}_p[u_\ell, u_r]$ consists of two waves (a 1-wave and a 2-wave) at most. Moreover, if u_ℓ is subsonic, i.e., $v(u_\ell) < a$, then it satisfies **(I)** and $\rho_\ell \in [\check{\rho}(0, u_r), \rho^a)$.

Proof. We first note that to have **(i)**, **(ii)** we need $q_\ell \geq 0$. If u_ℓ satisfies **(I)** and $u_\ell \neq u_r$, then $\mathcal{RS}_p[u_\ell, u_r]$ has only a 2-wave with strictly positive speed; otherwise $u_\ell = u_r$ and we have $\mathcal{RS}_p[u_\ell, u_r] \equiv u_r$. In both cases **(i)** and **(ii)** follow. If u_ℓ satisfies **(II)** but not **(I)**, then $\mathcal{RS}_p[u_\ell, u_r]$ has a 1-wave with strictly positive speed from u_ℓ to $\tilde{u}(u_\ell, u_r)$ and, if $\tilde{u}(u_\ell, u_r) \neq u_r$, it also has a 2-wave with strictly positive speed; again **(i)** and **(ii)** follow. If u_ℓ satisfies **(III)**, then $\mathcal{RS}_p[u_\ell, u_r]$ has a 1-shock with strictly positive speed from u_ℓ to $\tilde{u}(u_\ell, u_r)$ and, if $\tilde{u}(u_\ell, u_r) \neq u_r$, also a 2-wave with strictly positive speed; again **(i)** and **(ii)** follow.

Assume **(i)** and **(ii)**. By the construction of \mathcal{RS}_p , **(i)** implies that $\mathcal{RS}_p[u_\ell, u_r](0) = u_\ell$ and hence, since \mathcal{RS}_p is consistent, $\mathcal{RS}_p[u_\ell, u_r](\xi) = u_\ell$ for any $\xi \leq 0$, hence **(ii)** implies that $q_\ell \geq 0$. It is then easy to prove that **(I)**-**(III)** describe the only possible cases to have **(i)** and **(ii)**.

We now prove the last statement. If u_ℓ is subsonic, then by (b) in Proposition 2.7 and the fact that $\mathcal{RS}_p[u_\ell, u_r]$ has only waves with non-negative speed it follows that $\mathcal{RS}_p[u_\ell, u_r]$ has no 1-waves, and then $u_\ell \in \text{BL}_2^{u_r}$. Moreover $\rho_\ell \geq \check{\rho}(0, u_r)$ because $q_\ell \geq 0$, and $\rho_\ell < \rho^a$ because u_ℓ is subsonic. \square

In analogy to (2.14), for $u_r \in \Omega$ with $q_r \geq 0$, we denote

$$\Gamma_o^+(u_r) \doteq \{u_\ell \in \Omega : u_\ell \text{ satisfies one of conditions (I)-(III) in Corollary 2.11}\}. \quad (2.15)$$

Denote the lower boundary of the set identified by **(III)** in Corollary 2.11 with $B^+(u_r)$.

2.3.3 Demand and supply functions

The *demand* and *supply* functions $\bar{Q}, \underline{Q} : \Omega \rightarrow \mathbb{R}$ are defined as follows:

$$\bar{Q}(\rho, q) \doteq \begin{cases} q & \text{if } \rho < \bar{\rho}(\rho, q), \\ \bar{q}(\rho, q) & \text{if } \rho \geq \bar{\rho}(\rho, q), \end{cases} \quad \underline{Q}(\rho, q) \doteq \begin{cases} q & \text{if } \rho < \underline{\rho}(\rho, q), \\ \underline{q}(\rho, q) & \text{if } \rho \geq \underline{\rho}(\rho, q). \end{cases} \quad (2.16)$$

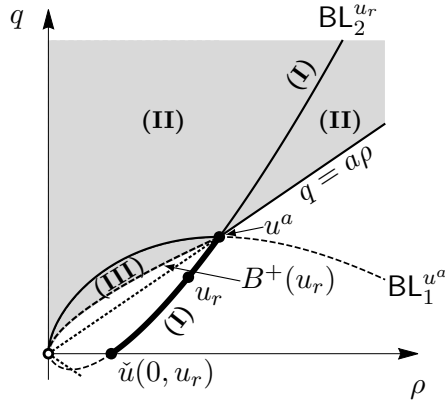


Figure 7: The set $\Gamma_o^+(u_r)$ (shaded regions, solid lines and the full points, but not the dashed lines) in (2.15).

They were introduced in [23] for the flow in Godunov's scheme. These functions are referred to as the *sending capacity* and *receiving capacity*, respectively, in the framework of traffic modeling, see [10]. The functions \bar{Q} and \underline{Q} have the following properties, which follow from Lemma 2.1.

Lemma 2.12. *We have $\bar{Q}, \underline{Q} \in \mathbf{C}^1(\Omega)$ and, for any $u \in \Omega$,*

$$\underline{q}(u) \leq \underline{Q}(u) < 0 < \bar{Q}(u) \leq \bar{q}(u). \quad (2.17)$$

We now provide a motivation for the introduction of $\bar{Q}(u_\ell)$ and $\underline{Q}(u_\ell)$.

Proposition 2.13. *$\bar{Q}(u_\ell)$ is the maximum flow attainable by $\mathcal{RS}_p[u_\ell, u_r](0)$ for any $u_r \in \Omega$; $\underline{Q}(u_r)$ is the minimum flow attainable by $\mathcal{RS}_p[u_\ell, u_r](0)$ for any $u_\ell \in \Omega$.*

Proof. We only prove the first statement. Note that by (2.5) we have $q_p^- = q_p^+$. It is not restrictive to assume that $\mathcal{RS}_p[u_\ell, u_r]$ has only waves with non-positive speeds and $\mathcal{RS}_p[u_\ell, u_r](0^-) = u_r$.

- Assume that $\rho_\ell < \bar{\rho}(u_\ell)$; in this case we have $q_\ell > 0$ and $\bar{Q}(u_\ell) = q_\ell$. We claim that $q_r \leq q_\ell$. In fact:
 - if $\mathcal{RS}_p[u_\ell, u_r]$ has a 2-wave, then by (a) in Proposition 2.7 we have $q_r < 0$ and therefore $q_r < 0 < q_\ell$;
 - if $\mathcal{RS}_p[u_\ell, u_r]$ has only a 1-wave, then it must be a 1-shock with $q_\ell > q_r$;
 - if $\mathcal{RS}_p[u_\ell, u_r]$ is constant, then $q_r = q_\ell$.
- Assume that $\rho_\ell \geq \bar{\rho}(u_\ell)$; in this case $\bar{Q}(u_\ell) = \bar{q}(u_\ell) \geq 0$. We claim that $q_r \leq \bar{q}(u_\ell)$. In fact:
 - if $\mathcal{RS}_p[u_\ell, u_r]$ has a 2-wave, then by (a) in Proposition 2.7 we have that $q_r < 0$ and so $q_r < 0 \leq \bar{q}(u_\ell)$;
 - if $\mathcal{RS}_p[u_\ell, u_r]$ has only a 1-wave, then either it is a 1-shock with $\rho_\ell < \rho_r$ and $q_r < q_\ell \leq \bar{q}(u_\ell)$, or it is a 1-rarefaction with $\bar{\rho}(u_\ell) \leq \rho_r < \rho_\ell$ and $q_\ell < q_r \leq \bar{q}(u_\ell)$;
 - if $\mathcal{RS}_p[u_\ell, u_r]$ is constant, then $q_r = q_\ell \leq \bar{q}(u_\ell)$.

This concludes the proof of the first statement. \square

Remark 2.14.

- (i) By (2.16) and (2.17) we deduce $\bar{Q}(u_\ell) \geq q_\ell$, $0 < \bar{Q}(u_\ell) \leq \bar{q}(u_\ell)$, $\underline{Q}(u_r) \leq q_r$ and $0 > \underline{Q}(u_r) \geq \underline{q}(u_r)$. So, if $q_o \in [\underline{Q}(u_r), \bar{Q}(u_\ell)]$, then $\hat{u}(q_o, u_\ell)$ and $\tilde{u}(q_o, u_r)$ are well defined.
- (ii) The states $\hat{u} = \hat{u}(q_o, u_\ell)$ and $\tilde{u} = \tilde{u}(q_o, u_r)$ are well defined if $q_o \in [\underline{q}(u_r), \bar{q}(u_\ell)]$. Observe that $[\underline{Q}(u_r), \bar{Q}(u_\ell)] \subseteq [\underline{q}(u_r), \bar{q}(u_\ell)]$ by (2.17). Moreover, the stricter condition $q_o \in [\underline{q}(u_r), \bar{Q}(u_\ell)]$ ensures that $\xi \mapsto \mathcal{RS}_p[u_\ell, \hat{u}](\xi) \in \text{FL}_1^{u_\ell}$ is formed at most by a single 1-wave with non-positive speed. Analogously, condition $q_o \in [\underline{Q}(u_r), \bar{q}(u_\ell)]$ ensures that $\xi \mapsto \mathcal{RS}_p[\tilde{u}, u_r](\xi) \in \text{FL}_2^{\tilde{u}}$ consists at most of a single 2-wave with non-negative speed.

3 Self-similar c-Riemann solvers

In this section we introduce the modeling of a gas flow through a *coupling*.

3.1 General definition and main properties

The following definition introduces the notion of coupling Riemann solver, where the coupling takes place at $x = 0$. A key feature of the solver is that the traces $q(0^\pm, t)$ of the momentum are equal for every $t \geq 0$; this common value, which depends on the initial data u_ℓ and u_r of the Riemann problem, is denoted by q_c^0 , and ranges in $[Q(u_r), \bar{Q}(u_\ell)]$ because of Proposition 2.13. Also the traces $\rho(0^\pm, t)$ at 0 of the density, denoted below by ρ_c^\pm , depend on u_ℓ, u_r .

Definition 3.1. *Let $D_c \subseteq D$ be non-empty. A function*

$$C: \quad D_c \quad \rightarrow \quad D \\ (u_\ell, u_r) \quad \mapsto \quad (u_c^-(u_\ell, u_r), u_c^+(u_\ell, u_r))$$

is a coupling function if there exist $\rho_c^-, \rho_c^+ : D_c \rightarrow (0, \infty)$ and $q_c^0 : D_c \rightarrow \mathbb{R}$ such that $u_c^- = (\rho_c^-, q_c^0)$, $u_c^+ = (\rho_c^+, q_c^0)$ and for any $(u_\ell, u_r) \in D_c$ we have

$$u_c^-(u_\ell, u_r) \in \Gamma^-(u_\ell), \quad u_c^+(u_\ell, u_r) \in \Gamma^+(u_r). \quad (3.1)$$

The corresponding c-Riemann solver $\mathcal{RS}_c : D_c \rightarrow \mathbf{BV}(\mathbb{R}; \Omega)$ is defined as

$$\mathcal{RS}_c[u_\ell, u_r](\xi) \doteq \begin{cases} \mathcal{RS}_p[u_\ell, u_c^-](\xi) & \text{if } \xi < 0, \\ \mathcal{RS}_p[u_c^+, u_r](\xi) & \text{if } \xi \geq 0, \end{cases} \quad (u_c^-, u_c^+) = C(u_\ell, u_r). \quad (3.2)$$

In analogy with (2.7), we denote

$$u_c \doteq (\rho_c, q_c) \doteq \mathcal{RS}_c[u_\ell, u_r], \quad u_c^\pm \doteq (\rho_c^\pm, q_c^0) \doteq u_c(0^\pm).$$

Remark 3.2. We now comment on Definition 3.1 and introduce some notation.

- (i) The map $(t, x) \mapsto \mathcal{RS}_c[u_\ell, u_r](x/t)$ is an entropy solution to (2.1) in $x < 0$ and $x > 0$ and satisfies the first Rankine-Hugoniot condition (2.5) at $x = 0$, see [45]. Condition (2.5) is always satisfied by u_c : if u_c has a *stationary* discontinuity at $x = 0$, then $\dot{\gamma} = 0$ but u_c^- and u_c^+ have the same flux q_c^0 , and so (2.5) holds. On the contrary, u_c may not satisfy the second Rankine-Hugoniot condition (2.6) at $x = 0$, hence conservation of momentum may be lost at $x = 0$. Then, u_c may fail to be a weak solution of (2.1) in the whole of \mathbb{R} .
- (ii) A c-Riemann solver \mathcal{RS}_c is uniquely characterized by the function C , which associates to the initial values (2.4) the traces u_c^\pm of the solution u_c at $\xi = 0^\pm$. For brevity we omitted the dependence of \mathcal{RS}_c on C . In the literature, C is usually given implicitly by imposing some conditions on the traces u_c^- and u_c^+ . This leads to two issues: to search for which Riemann initial data (u_ℓ, u_r) the traces u_c^- and u_c^+ exist and, in such a case, if such traces are uniquely determined. At last, condition (3.1) is typically omitted.
- (iii) By the definitions (2.12), (2.13) of $\Gamma^-(u_\ell)$ and $\Gamma^+(u_r)$, condition (3.1) implies that for any $(u_\ell, u_r) \in D_c$ the following conditions are satisfied by $u_c^- = u_c^-(u_\ell, u_r)$ and $u_c^+ = u_c^+(u_\ell, u_r)$:
 - a) $\mathcal{RS}_p[u_\ell, u_c^-]$ has only waves with non-positive speed and $\mathcal{RS}_p[u_\ell, u_c^-](0^-) = u_c^-$;
 - b) $\mathcal{RS}_p[u_c^+, u_r]$ has only waves with non-negative speed and $\mathcal{RS}_p[u_c^+, u_r](0^+) = u_c^+$.
- (iv) The standard Riemann solver \mathcal{RS}_p is the c-Riemann solver corresponding to $C(u_\ell, u_r) \doteq (\mathcal{RS}_p[u_\ell, u_r](0^-), \mathcal{RS}_p[u_\ell, u_r](0^+))$ defined in $D_c \doteq D$. Moreover, $\mathcal{RS}_p[u_\ell, u_c^-](\xi) = u_c^-$ for every $\xi \geq 0$ by (iii)a) and $\mathcal{RS}_p[u_c^+, u_r](\xi) = u_c^+$ for every $\xi \leq 0$ by (iii)b). In particular, both $\mathcal{RS}_p[u_\ell, u_c^-]$ and $\mathcal{RS}_p[u_c^+, u_r]$ are continuous at $\xi = 0$.
- (v) If the flow is one-way, then $D_c \subseteq \{(u_\ell, u_r) \in D : q_\ell, q_r \geq 0\}$ and (3.1) is substituted with

$$u_c^-(u_\ell, u_r) \in \Gamma_o^-(u_\ell), \quad u_c^+(u_\ell, u_r) \in \Gamma_o^+(u_r). \quad (3.3)$$

The domain D_c of \mathcal{RS}_c can be strictly included in D . From a physical point of view, D_c represents the Riemann data belonging to the operating range of the coupling. The coupling may be either *inactive* or *active* according to the initial data. In the former case, the bare system (2.1) is sufficient to describe the flow in the whole of \mathbb{R} : no additional condition is imposed, the flow takes place exactly as if the coupling is missing, and the solution is provided by the standard Riemann solver \mathcal{RS}_p , that is $\mathcal{RS}_c[u_\ell, u_r] \equiv \mathcal{RS}_p[u_\ell, u_r]$. In the latter case, the coupling may be thought to act as an exterior force on the flow (think for instance at the case of a valve or a compressor) and then the conservation of momentum may be lost. Since the conservation of the mass still occurs, then only the first Rankine-Hugoniot condition (2.5) is imposed at $x = 0$.

We denote by $A \subseteq D_c$ the set of Riemann data for which the coupling is active. The set $D_c \setminus A$ is the set of Riemann data for which the coupling is inactive. Note that there may exist initial data $(u_\ell, u_r) \in A$ such that $u_c \equiv u_p$; this leads to define

$$A_N \doteq \left\{ (u_\ell, u_r) \in A : u_c \equiv u_p \right\}, \quad A_I \doteq A \setminus A_N.$$

The sets A_N and A_I are constituted by the Riemann data that make the coupling active and either do *not* influence or *influence* the flow, respectively. Obviously $\{(u_\ell, u_r) \in D_c : u_c \equiv u_p\} = D_c \setminus A_I$.

By Lemma 2.12 we have $0 \in [\underline{Q}(u_\ell), \overline{Q}(u_r)]$ for every $(u_\ell, u_r) \in D$. We say that for $(u_\ell, u_r) \in A$ the coupling is *closed* if $q_c^0 = 0$ and *open* if $q_c^0 \neq 0$. Notice that $q_c^0 = 0$ implies neither that the coupling is closed nor that it is active: for instance, if the coupling is inactive and $\tilde{q}(u_\ell, u_r) = 0$ then $q_c^0 = 0$.

In the following proposition we give two sufficient conditions on (u_ℓ, u_r) to have $u_c \equiv u_p$.

Proposition 3.3. *Fix $(u_\ell, u_r) \in D_c$. If either $u_c^- = u_c^+$ or $u_c^- = u_p^-$ and $u_c^+ = u_p^+$, then $u_c \equiv u_p$.*

Proof. We prove that if $u_c^- = u_c^+$, then $u_c \equiv u_p$. Let u_m be the common value of u_c^- and u_c^+ . We have $\mathcal{RS}_p[u_\ell, u_m](0) = u_m = \mathcal{RS}_p[u_m, u_r](0)$ by (iv) in Remark 3.2. Since \mathcal{RS}_p is consistent, it satisfies item **II.** in [14, page 713], hence

$$u_p(\xi) = \begin{cases} \mathcal{RS}_p[u_\ell, u_m](\xi) & \text{if } \xi < 0, \\ \mathcal{RS}_p[u_m, u_r](\xi) & \text{if } \xi \geq 0, \end{cases}$$

which coincides with u_c by (3.2).

We now prove that if $u_c^- = u_p^-$ and $u_c^+ = u_p^+$, then $u_c \equiv u_p$. By the first claim it is sufficient to consider the case $u_p^- \neq u_p^+$. Then, the proof shall follow from

$$u_p(\xi) = \begin{cases} \mathcal{RS}_p[u_\ell, u_p^-](\xi) & \text{if } \xi < 0, \\ \mathcal{RS}_p[u_p^+, u_r](\xi) & \text{if } \xi \geq 0, \end{cases}$$

which coincides with u_c by (3.2). We prove the above equality. By the symmetry of the problem, it is not restrictive to assume that u_p has a 1-shock at $\xi = 0$. Then $u_\ell = u_p^-$ and therefore $u_p(\xi) = \mathcal{RS}_p[u_\ell, u_p^-](\xi) = u_\ell$ for all $\xi < 0$. If $u_r = u_p^+$, then $u_p(\xi) = \mathcal{RS}_p[u_p^+, u_r](\xi) = u_r$ for all $\xi > 0$. Assume that $u_r \neq u_p^+$. In this case u_p has in $\xi > 0$ a 2-wave between u_p^+ and u_r . Therefore, we have $u_p(\xi) = \mathcal{RS}_p[u_p^+, u_r](\xi)$ for all $\xi > 0$. This concludes the proof. \square

Proposition 3.3 can be rephrased as

$$\left\{ (u_\ell, u_r) \in A : u_c^- = u_c^+ \right\} \cup \left\{ (u_\ell, u_r) \in A : u_c^- = u_p^- \text{ and } u_c^+ = u_p^+ \right\} \subseteq A_N.$$

In Proposition 4.5 we show that also the coupling condition (4.7) implies $u_c \equiv u_p$; in that case the assumptions of Proposition 3.3 are not satisfied.

3.2 Waves of c-Riemann solvers

The following proposition states that $\mathcal{RS}_c[u_\ell, u_r]$ admits at most four waves; we refer to Subsection 5.2 for an explicit example. More precisely, two Lax waves in $x > 0$ appear if $q_c^0 > 0$, and in $x < 0$ if $q_c^0 < 0$. By the way, this is the reason why $\mathcal{RS}_c[u_\ell, u_r]$ cannot be formed by five waves. We defer to Figure 11 for a numerical example of a solution with four waves.

Proposition 3.4. *The function $\xi \mapsto u_c(\xi) \doteq \mathcal{RS}_c[u_\ell, u_r](\xi)$ can involve up to four waves (including the stationary discontinuity at $\xi = 0$). Furthermore:*

$$q_c^0 \in [Q(u_r), \bar{Q}(u_\ell)], \quad (3.4)$$

$$\left\| u_c^- - \hat{u}(q_c^0, u_\ell) \right\| \cdot \left\| u_c^+ - \check{u}(q_c^0, u_r) \right\| = 0. \quad (3.5)$$

Moreover:

i) u_c has two waves in $\xi < 0$ if and only if $\rho_c^- \leq \underline{\rho}(u_c^-)$ and $(\bar{\rho}(u_\ell, u_c^-) - \rho_c^-)(\tilde{q}(u_\ell, u_c^-) - q_c^0) < 0$; this implies

$$u_c^- \neq \hat{u}(q_c^0, u_\ell), \quad v(u_c^-) \leq -a, \quad q_c^0 < 0, \quad \tilde{q}(u_\ell, u_c^-) < 0.$$

ii) u_c has two waves in $\xi > 0$ if and only if $\rho_c^+ \leq \bar{\rho}(u_c^+)$ and $(\bar{\rho}(u_c^+, u_r) - \rho_c^+)(\tilde{q}(u_c^+, u_r) - q_c^0) > 0$; this implies

$$u_c^+ \neq \check{u}(q_c^0, u_r), \quad v(u_c^+) \geq a, \quad q_c^0 > 0, \quad \tilde{q}(u_c^+, u_r) > 0.$$

Proof. We divide the proof in some steps.

- First, we show for which initial data (u_ℓ, u_r) the solution u_c has four waves, and prove that u_c cannot have more than four waves.
 - a)** By definition, $\mathcal{RS}_p[u_\ell, u_c^-]$ has at most two waves: the first is the 1-wave $\mathcal{RS}_p[u_\ell, \tilde{u}(u_\ell, u_c^-)]$ and the second is the 2-wave $\mathcal{RS}_p[\tilde{u}(u_\ell, u_c^-), u_c^-]$. If both waves have non-positive speed and $\mathcal{RS}_p[\tilde{u}(u_\ell, u_c^-), u_c^-](0^-) = u_c^-$, then $q_c^0 < 0$ by (a) in Proposition 2.7.
 - b)** Analogously, if $\mathcal{RS}_p[u_c^+, u_r]$ has two waves with non-negative speed and $\mathcal{RS}_p[u_c^+, u_r](0^+) = u_c^+$, then $q_c^0 > 0$ by (b) in Proposition 2.7.

Now, to conclude the proof of the first statement it is sufficient to observe that the above cases **a)** and **b)** cannot happen at the same time.

- To prove (3.4) it is sufficient to recall that $q_c^0 \in [Q(u_r), \bar{Q}(u_\ell)]$ by Proposition 2.13.
- We now prove (3.5). If $u_c^- = \hat{u}(q_c^0, u_\ell)$, then (3.5) is satisfied. Assume that $u_c^- \neq \hat{u}(q_c^0, u_\ell)$. In this case $\mathcal{RS}_p[u_\ell, u_c^-]$ has a possibly null 1-wave $(u_\ell, \tilde{u}(u_\ell, u_c^-))$ and a 2-wave $(\tilde{u}(u_\ell, u_c^-), u_c^-)$ with $q_c^0 < 0$, see the proof of Proposition 2.7. This implies that $u_c^+ = \check{u}(q_c^0, u_r)$ and (3.5) is satisfied.
- We now prove **i)**. Clearly, u_c has two waves in $\xi < 0$ if and only if $\mathcal{RS}_p[u_\ell, u_c^-]$ involves a 2-wave with negative speed, and therefore $u_c^- \neq \hat{u}(q_c^0, u_\ell)$. By (3.1)₁ we have $\mathcal{RS}_p[u_\ell, u_c^-](0^-) = u_c^-$. Hence, to complete the proof it is sufficient to apply item (a) in Proposition 2.7.
- At last, the proof of **ii)** is analogous to that of **i)** and is therefore omitted. \square

By (3.5) we have that if $u_c^- \neq \hat{u}(q_c^0, u_\ell)$ then $u_c^+ = \check{u}(q_c^0, u_r)$. The former condition implies that u_c^- does not belong to $\text{FL}_1^{u_\ell}$, hence $\mathcal{RS}_p[u_\ell, u_c^-]$ has two waves (a 1-wave and a 2-wave) at most, while the latter implies that u_c^+ belongs to $\text{BL}_2^{u_r}$, hence $\mathcal{RS}_p[u_c^+, u_r]$ has one wave (a 2-wave) at most. Analogous considerations hold in the case $u_c^+ \neq \check{u}(q_c^0, u_r)$.

In the following corollaries we provide sufficient conditions to have u_c with at most three waves. We shall exploit Corollary 3.6 when dealing with *compressors* in Section 6.2; this motivates the hypothesis (3.6).

Corollary 3.5. *If the flow is subsonic at $x = 0$, i.e., $|v(u_c^\pm)| < a$, then the function $\xi \mapsto u_c(\xi) \doteq \mathcal{RS}_c[u_\ell, u_r](\xi)$ can involve up to three waves (including the stationary discontinuity at $\xi = 0$); in this case u_c consists of a 1-wave in $\xi < 0$ and a 2-wave in $\xi > 0$.*

Proof. It simply follows from Proposition 3.4. \square

Corollary 3.6. Fix (u_ℓ, u_r) in D_c . If the flow is one-way, say $q_c \geq 0$ in \mathbb{R} , and

$$\rho_c^- < \rho_c^+, \quad (3.6)$$

then u_c has at most three waves (including the stationary discontinuity at $\xi = 0$). Moreover, one of the following mutually exclusive conditions is satisfied:

- (1) u_ℓ is supersonic, $u_c^- = u_\ell$ and $u_c^+ \in \Gamma_o^+(u_r)$;
- (2) $u_c^- \in \Gamma_o^-(u_\ell)$ is non-supersonic and $u_c^+ \in \text{BL}_2^{u_r}$.

In case (1) we have u_c is constant in $\xi < 0$ and has at most two waves in $\xi > 0$. In case (2) we have that u_c has at most one wave for each side $\xi < 0$ and $\xi > 0$.

In both cases, u_c has always a stationary discontinuity at $\xi = 0$, at most one wave in $\xi < 0$ (a 1-wave) and at most three waves in \mathbb{R} . In particular, u_c^- is supersonic if and only if $u_\ell = u_c^-$ and u_ℓ is supersonic, i.e., in case (1).

Proof. Assume by contradiction that $\mathcal{RS}_c[u_\ell, u_r]$ has four waves. By hypothesis $q_c^0 \geq 0$, hence $\mathcal{RS}_p[u_\ell, u_c^-]$ has precisely a 1-wave by Proposition 3.4, item **i**). In particular, this implies that $u_\ell \neq u_c^-$ and that $\mathcal{RS}_p[u_c^+, u_r]$ has exactly two waves. By Proposition 3.4, item **ii**), we have that u_c^+ is non-subsonic, i.e., $v(u_c^+) \geq a$. This implies that u_c^- is supersonic because $v(u_c^+)/v(u_c^-) = \rho_c^-/\rho_c^+ < 1$ by (3.6). By the last statement in Corollary 2.10 with u_c^- in place of u_r , this implies that $u_\ell = u_c^-$, which gives a contradiction. This proves the first claim of the corollary.

Now, we prove that either (1) or (2) holds. We distinguish the following cases.

- Assume u_ℓ is supersonic. We have two possible situations.
 - If $u_c^- = u_\ell$, then $u_c^+ \in \Gamma_o^+(u_r)$ by (2.15) and Corollary 2.11 with u_c^+ in place of u_ℓ . This implies (1). In this case, we have no waves in $\xi < 0$, a stationary discontinuity at $\xi = 0$ and at most two waves in $\xi > 0$.
 - If $u_c^- \neq u_\ell$, then $\rho_c^- \in (\hat{\rho}(q_\ell, u_\ell), \hat{\rho}(0, u_\ell)]$ by (I) in Corollary 2.10 with u_c^- in place of u_r . By Proposition 2.5, this implies that u_c^- is subsonic. Moreover, by (3.6) also u_c^+ is subsonic; then, $u_c^+ \in \text{BL}_2^{u_r}$ with $\rho_c^+ \in [\check{\rho}(0, u_r), \rho^a(u_r))$ by the last statement in Corollary 2.11 with u_c^+ in place of u_ℓ . This implies (2). In this case, we have a 1-shock in $\xi < 0$, a stationary discontinuity at $\xi = 0$ and at most one wave in $\xi > 0$ (a 2-wave).
- Assume u_ℓ is non-supersonic. In this case also $u_c^- \in \Gamma_o^-(u_\ell)$ is non-supersonic by the last statement in Corollary 2.10, see Figure 6 on the right; hence u_c^+ is subsonic by (3.6) and therefore $u_c^+ \in \text{BL}_2^{u_r}$ with $\rho_c^+ \in [\check{\rho}(0, u_r), \rho^a(u_r))$ by the last statement in Corollary 2.11 with u_c^+ in place of u_ℓ . This implies (2). In this case, we have a 1-wave in $\xi < 0$, a stationary discontinuity at $\xi = 0$ and at most one wave in $\xi > 0$ (a 2-wave).

The last statement directly follows from the previous analysis. This concludes the proof. \square

3.3 Coherence of a c-Riemann solver

We can now give the definition of a *coherent* coupling Riemann solver.

Definition 3.7. A *c-Riemann solver* $\mathcal{RS}_c: D_c \rightarrow \mathbf{BV}(\mathbb{R}; \Omega)$ is coherent at $(u_\ell, u_r) \in D_c$ if the traces $u_c^\pm \doteq \mathcal{RS}_c[u_\ell, u_r](0^\pm)$ satisfy

$$(u_c^-, u_c^+) \in D_c \quad \text{and} \quad C(u_c^-, u_c^+) = (u_c^-, u_c^+).$$

The coherence domain CH of \mathcal{RS}_c is the set of all pairs $(u_\ell, u_r) \in D_c$ where \mathcal{RS}_c is coherent. The set $\text{CH}^c \doteq D_c \setminus \text{CH}$ is the incoherence domain.

A c-Riemann solver \mathcal{RS}_c is coherent at an initial datum $(u_\ell, u_r) \in D_c$ if the ordered pair of the traces of the corresponding solution $(u_c^-, u_c^+) \doteq (\mathcal{RS}_c[u_\ell, u_r](0^-), \mathcal{RS}_c[u_\ell, u_r](0^+))$ belongs to D_c and

is a fixed point of C ; in this case

$$\mathcal{RS}_c[u_c^-, u_c^+](\xi) = \begin{cases} u_c^- & \text{if } \xi < 0, \\ u_c^+ & \text{if } \xi \geq 0. \end{cases}$$

Hence, coherence may be thought as a stability property. On the contrary, for instance if the coupling represents a valve, the incoherence of a c-Riemann solver is understood as modeling the chattering and may yield analytical and numerical instabilities. We recall that an analogous condition (called however *consistency*) has been introduced in [30] at the junctions of a road network.

The Riemann solver \mathcal{RS}_p is coherent in D , see [19, Proposition 2.5]. On the contrary, coherence in D_c may fail for \mathcal{RS}_c because of the presence of the coupling, as we will see in Sections 5.2, 7 and 8. In the following theorem we give sufficient condition for the coherence of a c-Riemann solver. We recall the definitions (2.12), (2.13) of Γ^\pm and (2.14), (2.15) of Γ_\circ^\pm .

Theorem 3.8. *The c-Riemann solver \mathcal{RS}_c , associated to the coupling function C , is coherent in D_c if there exists $\pi: \Omega \rightarrow \Omega$ that satisfies the following conditions for any $(u_\ell, u_r) \in D_c$:*

- (1) $C(u_\ell, u_r) \in D_c$;
- (2) $(u^-, u^+) \in D_c$ is such that $(u^-, u^+) = C(u_\ell, u_r)$ if and only if $(u^-, u^+) \in \Gamma^-(u_\ell) \times \Gamma^+(u_r)$ and $u^+ = \pi(u^-)$;
- (3) there exists a unique pair $(u^-, u^+) \in \Gamma^-(u_\ell) \times \Gamma^+(u_r)$ such that $u^+ = \pi(u^-)$.

If the flow is one-way, then the same result holds by replacing $\Gamma^-(u_\ell) \times \Gamma^+(u_r)$ with $\Gamma_\circ^-(u_\ell) \times \Gamma_\circ^+(u_r)$.

Proof. Fix (u_ℓ, u_r) in D_c and consider $(u_c^-, u_c^+) = C(u_\ell, u_r)$. By (2.12), (2.13) and (2) we have $(u_c^-, u_c^+) \in \Gamma^-(u_c^-) \times \Gamma^+(u_c^+)$ and $u_c^+ = \pi(u_c^-)$. By (3), this implies that (u_c^-, u_c^+) is the unique pair in $\Gamma^-(u_c^-) \times \Gamma^+(u_c^+)$ such that $u_c^+ = \pi(u_c^-)$, hence by (1) and (2) we have $C(u_c^-, u_c^+) = (u_c^-, u_c^+)$.

The last statement can be proved analogously. This concludes the proof. \square

Note that item (1) in Theorem 3.8 implies that $C(D_c) \subseteq D_c$. By (2) and Definition 3.1, the second component of $\pi \doteq (\pi_1, \pi_2)$ coincides with the identity function: $\pi_2 \equiv \text{id}_{\mathbb{R}}$. At last item (3) can be rephrased as follows: the map $\pi: \Gamma^-(u_\ell) \rightarrow \Gamma^+(u_r)$ is injective.

4 Continuity conditions

In the following sections we recall some coupling conditions present in the literature and investigate their coherence. In this section we deal with conditions requiring the continuity either of the pressure, or of the dynamical pressure, or else of the specific enthalpy.

4.1 Continuity of the pressure

We begin with the coupling condition

$$p(\rho_c^+) = p(\rho_c^-), \tag{4.1}$$

which expresses the continuity of the pressure at $x = 0$, see for instance [1, (15b)], [4, (6)], [9, (A.2)], [17, (4.5)], [27, (8)], [31, (87)], [32, (11)], [33, (2.4)], [35, (2a)], [37, § 2.4], [39, (4.1)], [40, (8b)], [41, (C2)], [44, (3)], [46, (18)], [47, (34)], [50, (3.1)]. By (2.3), condition (4.1) implies the continuity of the density at $x = 0$, which in turn implies $u_c^- = u_c^+$. Therefore, the strong requirement (4.1) hides a smoothness assumption on the flow at $x = 0$.

By Proposition 3.3, the resulting c-Riemann solver \mathcal{RS}_c coincides with \mathcal{RS}_p in its domain of definition

$$D_c \doteq \{(u_\ell, u_r) \in D : \rho_p^+ = \rho_p^-\}, \tag{4.2}$$

which is strictly contained in the domain of definition D of \mathcal{RS}_p . Moreover, \mathcal{RS}_c is coherent in D_c because \mathcal{RS}_p is coherent in D .

Remark 4.1. Assumption (4.1) implies the entropy condition $\eta(u)_t + \phi(u)_x \leq 0$ in the distributional sense, for every pair (η, ϕ) , where η is a convex entropy for (2.1) and ϕ is the corresponding entropy flux, because \mathcal{RS}_p has this property and $\mathcal{RS}_c \equiv \mathcal{RS}_p$ in D_c . In the case of a general pressure law, an example is the pair (E, F) with

$$E(\rho, q) \doteq \frac{q^2}{2\rho} + \rho \int_{\rho_*}^{\rho} \frac{p(r)}{r^2} dr, \quad F(\rho, q) \doteq \frac{q}{\rho} (E(\rho, q) + p(\rho)), \quad (4.3)$$

where E is the *energy density* (E/ρ is the energy) and F its *flow*, see [16, page 1458], [17, page 609].

In the following proposition we show that the set D_c defined by (4.2) is not symmetric.

Proposition 4.2. *If $(u_1, u_2) \in D_c$, then (u_2, u_1) may well not belong to D_c .*

Proof. Consider $u_1, u_2 \in \Omega$ such that $u_2 \in \text{FL}_1^{u_1}$, $q_1 = q_2$ and $\rho_2 < \rho_1$. In this case $\mathcal{RS}_p[u_1, u_2]$ is a 1-rarefaction and $u_c^- = \bar{u}(u_1) = u_c^+$. This implies that $(u_1, u_2) \in D_c$. On the other hand, $\mathcal{RS}_p[u_2, u_1]$ is a 1-shock with $u_c^- = u_2 \neq u_c^+ = u_1$ and therefore $(u_2, u_1) \notin D_c$. This completes the proof. \square

4.2 Continuity of the dynamic pressure

The coupling condition

$$P(\rho_c^+, q_c^0) = P(\rho_c^-, q_c^0), \quad (4.4)$$

expresses the continuity of $P(u_c)$ at $\xi = 0$, where P is the dynamic pressure defined in (2.2), see [4, (7)] and [18, (10)]. Condition (4.4) corresponds to the second Rankine-Hugoniot condition (2.6) at $x = 0$. This implies that $(t, x) \mapsto u_c(x/t)$ is a weak solution in the sense of Definition 2.6, see [15, Proposition 1] for a detailed proof.

By (2.2) and (2.3), condition (4.4) is satisfied if and only if either $\rho_c^- = \rho_c^+$, i.e., $u_c^- = u_c^+$, or $\rho_c^- \neq \rho_c^+$ and

$$(q_c^0)^2 = a^2 \rho_c^- \rho_c^+. \quad (4.5)$$

The bare condition (4.5) implies that either both u_c^- and u_c^+ are sonic, or one is supersonic and the other is subsonic. As a consequence, if the flow is subsonic in \mathbb{R} , then (4.5) cannot hold, hence (4.4) implies $u_c^- = u_c^+$ and then $u_c \equiv u_p$ by Proposition 3.3.

However, for a general flow, (4.4) *does not select a unique c-Riemann solver*. For instance, if u_ℓ and u_r are as in Figure 8, left, then both u_p and u_c , represented in Figure 8 in the center and in the right, respectively, satisfy the coupling condition (4.4) and take the form (3.2). In Figure 8 we use the function $\pi: \Omega \rightarrow \Omega$ defined by

$$\pi(\rho, q) \doteq \left(\frac{v(\rho, q)^2}{a^2} \rho, q \right). \quad (4.6)$$

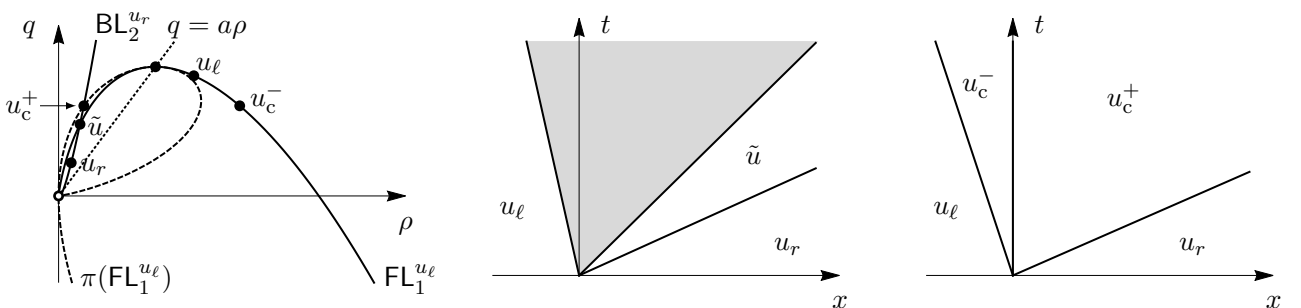


Figure 8: Two solutions satisfying (4.4). Above we denoted $\tilde{u} = \tilde{u}(u_\ell, u_r)$ and π is defined in (4.6). The solution in the center is the standard solution, whereas that on the right is not entropic.

In order to overcome the non-uniqueness of the c-Riemann solver, some authors have complemented

condition (4.4) with the coupling inequality

$$F(\rho_c^+, q_c^0) \leq F(\rho_c^-, q_c^0), \quad \text{for} \quad F(\rho, q) \doteq q \left(\frac{q^2}{2\rho^2} + a^2 \ln(\rho) \right). \quad (4.7)$$

Here F is the *flow of the energy density*, see (4.3)₂ with $\rho_* = e$, and plays the role of an entropy flow; see [15, Definition 1], [16, Definition 3.1], [17, Definitions 2.1 and 3.1 and (4.4)] and [50, Definition 1.2 and (3.3)]. Condition (4.7) is motivated by the usual entropy inequalities [7, § 4.4].

Remark 4.3. For a general gas, the flow F of the energy density is defined either in [15, (3)] or both in [16, page 1458] and [17, page 609], respectively, by

$$F(\rho, q) \doteq \frac{q}{\rho} \left(\frac{q^2}{2\rho} + \rho \int_{\rho_*}^{\rho} \frac{p'(r)}{r} dr \right), \quad F(\rho, q) \doteq \frac{q}{\rho} \left(\frac{q^2}{2\rho} + \rho \int_{\rho_*}^{\rho} \frac{p(r)}{r^2} dr + p(\rho) \right), \quad (4.8)$$

where $\rho_* > 0$ is a suitable constant. By taking $\rho_* = 1$ in (4.8)₁ and $\rho_* = e$ in (4.8)₂ we obtain (4.7).

Lemma 4.4. *The coupling condition (4.4), (4.7) holds true if and only if exactly one of the following conditions holds true:*

- (I) $u_c^- = u_c^+$;
- (II) $q_c^0 = -a\sqrt{\rho_c^- \rho_c^+}$ and $\rho_c^- > \rho_c^+$;
- (III) $q_c^0 = a\sqrt{\rho_c^- \rho_c^+}$ and $\rho_c^- < \rho_c^+$.

Proof. Recall that (4.4) is satisfied if and only if either $u_c^- = u_c^+$, or $u_c^- \neq u_c^+$ and (4.5) holds true. Note that if $u_c^- = u_c^+$, then both (4.7)₁ and (I) are satisfied, the former with the equality. Assume $u_c^- \neq u_c^+$ and (4.5). By (4.5) we have $q_c^0 \neq 0$ and from (4.7) we deduce

$$q_c^0 \left(\frac{\rho_c^+}{\rho_c^-} - \frac{\rho_c^-}{\rho_c^+} + 2 \ln \left(\frac{\rho_c^-}{\rho_c^+} \right) \right) \geq 0.$$

Observe that $r^{-1} - r + 2 \ln(r) > 0$ if and only if $r \in (0, 1)$. Hence, either (II) or (III) is satisfied. Finally, it is easy to show that (4.7) is satisfied if either (I)-(III) holds true. \square

We now show that the c-Riemann solver corresponding to (4.7) coincides with \mathcal{RS}_p ; as a consequence, the coupling function C implicitly defined by (4.7) is well defined in \mathbf{D} . This result extends to general flows that proved in [15, Proposition 1] for subsonic flows.

Proposition 4.5. *If \mathcal{RS}_c is the c-Riemann solver associated to (4.4), (4.7), then $\mathcal{RS}_c \equiv \mathcal{RS}_p$.*

Proof. Fix $(u_\ell, u_r) \in \mathbf{D}$. As already observed, $(t, x) \mapsto u_c(x/t)$ is a weak solution of (2.1), (2.4) in the sense of Definition 2.6. This implies that u_c has only waves of the first or second family. As a consequence u_c has at most two waves (a 1-wave followed by a 2-wave).

If $u_c^- = u_c^+$, then by Proposition 3.3 we have $u_c \equiv u_p$. Assume $u_c^- \neq u_c^+$, i.e., $\rho_c^- \neq \rho_c^+$. By the symmetry of the problem, it is not restrictive to assume that u_c has a 1-shock at $\xi = 0$. In this case $q_c^0 > 0$ because $u_c^+ \in \text{FL}_1^{u_c^-}$, hence by (III) in Lemma 4.4 we have $\rho_c^- < \rho_c^+$. Now, to conclude the proof, it is sufficient to observe that u_p is the unique weak solution which involves only waves of the first and second family, and such that the discontinuities of the first and second family are respectively increasing and decreasing in the ρ -coordinate. \square

Since \mathcal{RS}_p is coherent, hence the coupling (4.4), (4.7) ensures the *coherence* of the associated c-Riemann solver. A remark analogous to Remark 4.1 holds: condition (4.4) and the single ‘‘entropy condition’’ (4.7) imply the entropy condition $\eta(u)_t + \phi(u)_x \leq 0$ for every (η, ϕ) , with η convex.

4.3 Continuity of the specific enthalpy

The coupling condition

$$\mathcal{E}(u_c^+) = \mathcal{E}(u_c^-), \quad \text{for} \quad \mathcal{E}(u) \doteq \frac{v(u)^2}{2} + a^2 \ln(\rho), \quad (4.9)$$

expresses the continuity of the Bernoulli invariant according to [51, (4.2)] and of the specific stagnation enthalpy according to [28, (2.6)].

Proposition 4.6. *Condition (4.9) does not select a unique coupling function C in \mathcal{D} .*

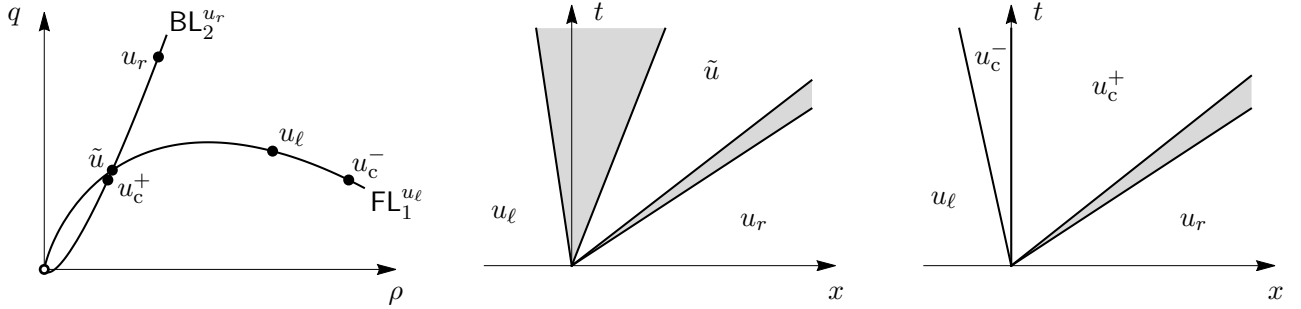


Figure 9: Two solutions satisfying the coupling condition (4.9). Above we denote $\tilde{u} = \tilde{u}(u_\ell, u_r)$. The standard solution is in the middle.

Proof. We first observe that (4.9) is equivalent to

$$\left(\frac{q_c^0}{a\rho_c^-} \right)^2 + 2 \ln(\rho_c^-) = \left(\frac{q_c^0}{a\rho_c^+} \right)^2 + 2 \ln(\rho_c^+),$$

with $q_c^0 = \text{FL}_1^{u_\ell}(\rho_c^-)$. For some values of ρ_c^- , such equation has two different solutions in ρ_c^+ , whose trivial one is $\rho_c^+ = \rho_c^-$. Indeed, if $q_c^0 \neq 0$ then the map $\rho \mapsto \mathfrak{B}(\rho) \doteq \left(\frac{q_c^0}{a\rho} \right)^2 + 2 \ln(\rho)$ satisfies

$$\lim_{\rho \rightarrow 0^+} \mathfrak{B}(\rho) = \infty, \quad \lim_{\rho \rightarrow \infty} \mathfrak{B}(\rho) = \infty, \quad \min \mathfrak{B} = 1 + 2 \ln(q_c^0/a),$$

and therefore it is sufficient to fix $\rho_c^- > 0$, compute q_c^0 and then take $\rho_c^+ \neq \rho_c^-$ such that $\mathfrak{B}(\rho_c^+) = \mathfrak{B}(\rho_c^-)$. This allows to construct two solutions for some values of $(u_\ell, u_r) \in \mathcal{D}$, see for instance Figure 9. \square

Remark 4.7. If $q_c^0 \neq 0$, then condition (4.9) is equivalent to $F(u_c^-) = F(u_c^+)$, for F defined in (4.7). In particular, (4.9) implies (4.7). If $q_c^0 > 0$ then condition (4.4), (4.7) implies $\rho_c^- \leq \rho_c^+$, see **(I)** and **(III)** in Lemma 4.4, while (4.9) does not ensure the inequality $\rho_c^- \leq \rho_c^+$, see for instance Figure 9.

Remark 4.8. In [50] it is considered the Euler equations (2.1) for an isentropic gas, i.e., $p(\rho) = a^2 \rho^\gamma$ with $\gamma > 1$; at the coupling the authors impose both the usual entropy inequality as well as the continuity of the specific enthalpy, see [50, (1.12) and (3.9)] or [49, (24)]. In the case of an isothermal gas, such conditions become (4.7) and (4.9), respectively. We already noticed that (4.9) implies (4.7); hence, also in this case we have no uniqueness for C in \mathcal{D} .

5 One-way flows

This section deals with the couplings introduced in [2]. We consider one-way flows, i.e., $q \geq 0$, see [2, (12b)]; moreover, the flow in the two pipes $x < 0$ and $x > 0$ is ruled by the pressure laws $p_1(\rho) \doteq a_1^2 \rho$ and $p_2(\rho) \doteq a_2^2 \rho$, respectively. This motivates the introduction of the notation \tilde{q}_{a_1} for

the function \tilde{q} defined in Definition 2.3 and corresponding to the sonic velocity $a = a_1$; an analogous notation is exploited for other quantities.

Two different coupling conditions are proposed. The first imposes that the flow along the outgoing pipe is not supersonic. The second requires the continuity of the pressure at $x = 0$, i.e., (4.1), and, among all the c-Riemann solvers satisfying such condition, it maximizes the flow across $x = 0$, see [2, (28)]. Both conditions uniquely selects a c-Riemann solver, but only the former is coherent. We describe in detail the two c-Riemann solvers in the following subsections.

5.1 Non-supersonic flow along the outgoing pipe

The first c-Riemann solver \mathcal{RS}_c defined in [2] corresponds to consider

$$D_c \doteq \{(u_\ell, u_r) \in D : q_\ell \geq 0, 0 \leq v(u_r) \leq a_2\} \quad (5.1a)$$

and, for all $(u_\ell, u_r) \in D_c$, to take

$$q_c^0 \doteq \min\{\bar{Q}_{a_1}(u_\ell), q^{a_2}(u_r)\}, \quad (5.1b)$$

$$u_c^- \doteq \begin{cases} u_\ell & \text{if } q_c^0 = q_\ell, \\ \hat{u}_{a_1}(q_c^0, u_\ell) & \text{if } q_c^0 \neq q_\ell, \end{cases} \quad u_c^+ \doteq \check{u}_{a_2}(q_c^0, u_r). \quad (5.1c)$$

About (5.1b), we note that $\bar{Q}_{a_1}(u_\ell) > 0$ by (2.17), for every $u_\ell \in \Omega$. Moreover, we have $q^{a_2}(u_r) > 0$ since it corresponds to the flux of the intersection of $\text{BL}_{2,a_2}^{u_r}$ with the sonic line $q = a_2\rho$, see Definition 2.3. As a consequence, q_c^0 is well defined, $q_c^0 > 0$ and u_c^+ is not supersonic by (5.1c)₂. By (5.1c), the corresponding c-Riemann solver is as follows. It has, at most, one wave in $\xi < 0$, namely a 1-wave, because either $u_c^- = u_\ell$ (and then no wave) or by definition of \hat{u} it has a 1-wave connecting u_ℓ with $\hat{u}_{a_1}(q_c^0, u_\ell)$; one wave at $\xi = 0$ (a stationary discontinuity); and one wave in $\xi > 0$ (a 2-wave), by definition of \check{u} .

It is easy to show that $v(\mathcal{RS}_c[u_\ell, u_r]) \geq 0$ in \mathbb{R} , i.e., the flow is one-way along both pipes, and $v(\mathcal{RS}_c[u_\ell, u_r](\xi)) \leq a_2$ for every $\xi > 0$, i.e., the flow is not supersonic along the outgoing pipe, see [2, (26)]. Some examples of solutions are presented in Figure 10.

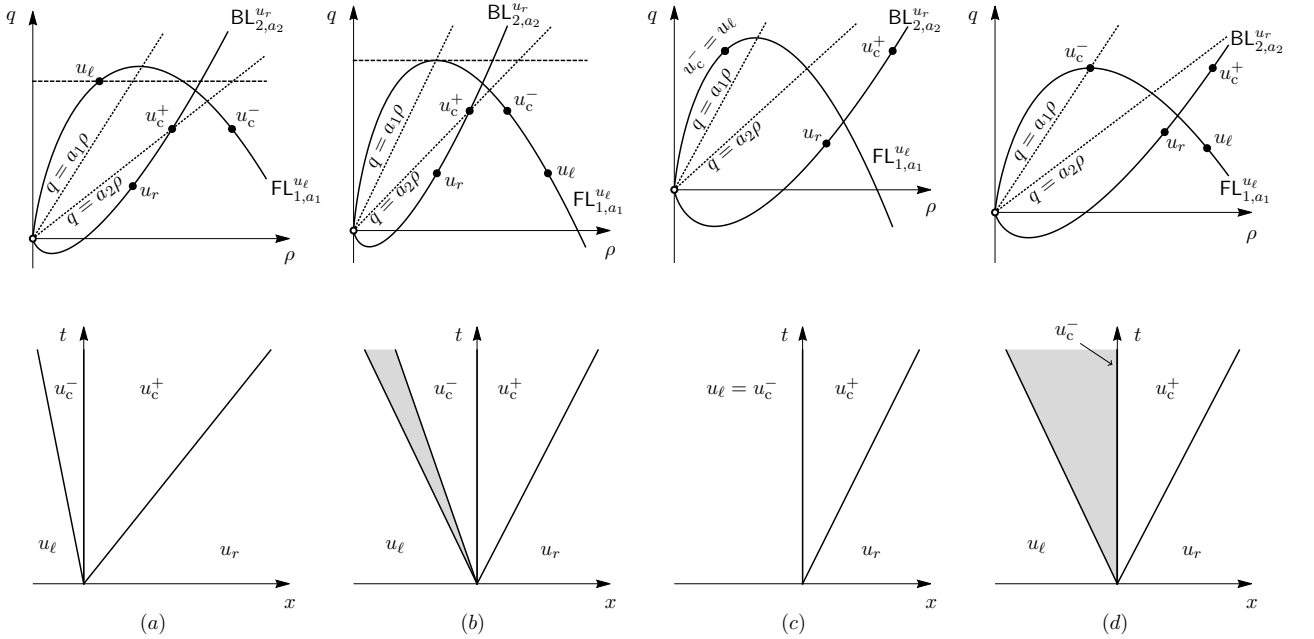


Figure 10: Examples of solutions corresponding to the c-Riemann solver in (5.1). Here $a_1 = 2$ and $a_2 = 1$.

Proposition 5.1. *The c-Riemann solver \mathcal{RS}_c corresponding to (5.1) is coherent.*

Proof. Fix $(u_\ell, u_r) \in D_c$. We already observed that $q_c^0 > 0$ and $v(u_c^+) \leq a_2$, hence $(u_c^-, u_c^+) \in D_c$.

To complete the proof it remains to show that $C(u_c^-, u_c^+) = (u_c^-, u_c^+)$; it is sufficient to prove

$$\min\{\overline{Q}_{a_1}(u_c^-), q^{a_2}(u_c^+)\} = q_c^0. \quad (5.2)$$

- If $q^{a_2}(u_r) \leq \overline{Q}_{a_1}(u_\ell)$, see Figure 10, (a) and (b), then u_c^+ is a sonic state; hence by (2.16) we have

$$q^{a_2}(u_c^+) = q_c^0 \leq \overline{Q}_{a_1}(u_c^-).$$

- If $q^{a_2}(u_r) > \overline{Q}_{a_1}(u_\ell)$ and u_ℓ is not a subsonic state, see Figure 10, (c), then $u_c^- = u_\ell$ is not a subsonic state and u_c^+ is a subsonic state; hence

$$q_\ell = \overline{Q}_{a_1}(u_c^-) = q_c^0 < q^{a_2}(u_c^+).$$

- If $q^{a_2}(u_r) > \overline{Q}_{a_1}(u_\ell)$ and u_ℓ is a subsonic state, see Figure 10, (d), then u_c^- is a sonic state and u_c^+ is a subsonic state; hence

$$q_\ell < \overline{Q}_{a_1}(u_c^-) = q_c^0 < q^{a_2}(u_c^+).$$

In any of the preceding three cases, formula (5.2) holds true. This concludes the proof. \square

The previous proposition obviously holds in the case of a single pressure law, i.e., $a_1 = a_2$.

5.2 Continuity of the pressure

A second c-Riemann solver is proposed in [2], which is extended to the case of a network in [3] and to general flows in [11, § 4]. For $(u_\ell, u_r) \in D$ with $q_\ell, q_r \geq 0$, we denote by $\mathfrak{Q}(u_\ell, u_r)$ the set of $q \in [0, \overline{Q}_{a_1}(u_\ell)]$ such that $(\rho, q) \doteq \mathcal{RS}_{p, a_1}[u_\ell, \hat{u}_{a_1}(q, u_\ell)](0^-)$ satisfies the following conditions:

$$\mathcal{RS}_{p, a_2}\left[\left(\frac{a_1^2}{a_2^2}\rho, q\right), u_r\right](0^+) = \left(\frac{a_1^2}{a_2^2}\rho, q\right), \quad \tilde{q}_{a_2}\left(\left(\frac{a_1^2}{a_2^2}\rho, q\right), u_r\right) \geq 0. \quad (5.3)$$

Then we denote

$$D_c \doteq \{(u_\ell, u_r) \in D : q_\ell, q_r \geq 0, \mathfrak{Q}(u_\ell, u_r) \neq \emptyset\}, \quad (5.4)$$

and, for all $(u_\ell, u_r) \in D_c$, we define

$$q_c^0 \doteq \max \mathfrak{Q}(u_\ell, u_r), \quad u_c^- \doteq \mathcal{RS}_{p, a_1}[u_\ell, \hat{u}_{a_1}(q_c^0, u_\ell)](0^-), \quad u_c^+ \doteq \left(\frac{a_1^2}{a_2^2}\rho_c^-, q_c^0\right). \quad (5.5)$$

By construction we have $q_c^0 \geq 0$, hence Proposition 2.7 ensures that $\xi \mapsto \mathcal{RS}_c[u_\ell, u_r](\xi)$ has at most one wave in $\xi < 0$ (a 1-wave connecting u_ℓ to $u_c^- = \hat{u}_{a_1}(q_c^0, u_\ell)$), one wave at $\xi = 0$ (a stationary discontinuity) and up to two waves in $\xi > 0$ (a 1-wave followed by a 2-wave).

As a result, $\xi \mapsto \mathcal{RS}_c[u_\ell, u_r]$ can involve up to four waves, see Propositions 3.4. The numerical example presented in Figure 11 shows that this is the case if we choose $u_\ell = (15, 0)$, $u_r = (10, 24)$, and the sound speeds $a_1 = 1$, $a_2 = 2$. Indeed, we see a 1-rarefaction at $x < 0$, a stationary discontinuity at $x = 0$, followed by a 1-shock close to $x = 0$ and then by a 2-rarefaction.

For the numerical simulations presented in Figures 11 and 15, we employ the Glimm scheme [13, 54], which has also been applied to c-Riemann solvers in [20]. Throughout all simulations, we adopt a spatial discretization of $\Delta x = 10^{-4}$, and the time discretization is determined by considering the CFL condition, with a fixed CFL value of 0.45.

The main properties of \mathcal{RS}_c are:

- $v(\mathcal{RS}_c[u_\ell, u_r]) \geq 0$ in \mathbb{R} , because $q_\ell, q_c^0, q_r \geq 0$, i.e., the flow is one-way along the two pipes;
- $p_{a_1}(\rho_c^-) = p_{a_2}(\rho_c^+)$, i.e., the pressure is continuous at $\xi = 0$, namely $a_1^2 \rho_c^- = a_2^2 \rho_c^+$, see [2, (27)].

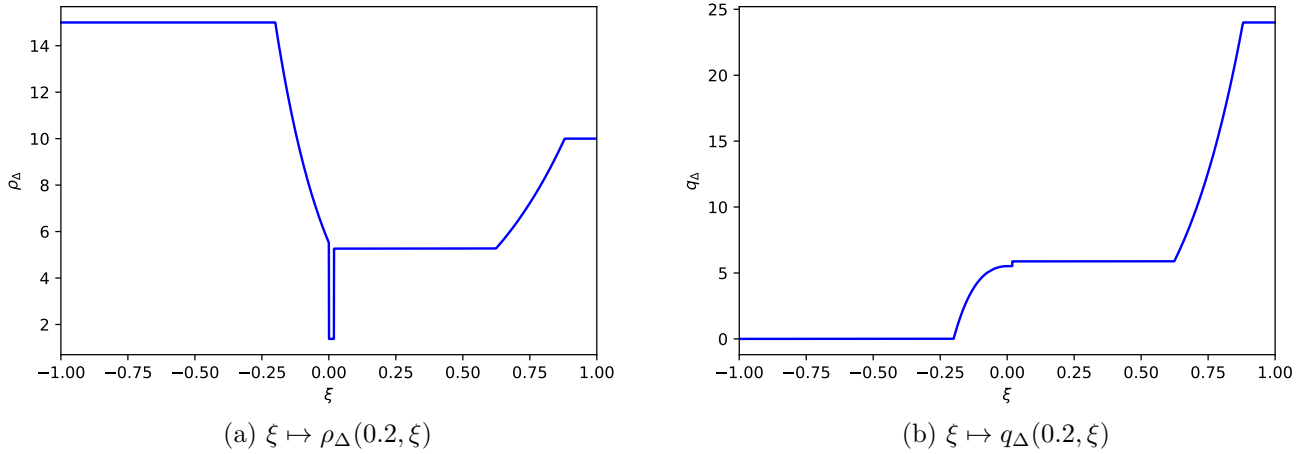


Figure 11: An example of a numerical solution with four waves.

We can now exploit Corollaries 2.10 and 2.11 to give a more explicit characterization of D_c . To this aim, let $\pi: \Omega \rightarrow \Omega$ be defined by

$$\pi(\rho, q) \doteq \left(\frac{a_1^2}{a_2^2} \rho, q \right).$$

Then, we can write D_c defined in (5.4) as

$$D_c = \left\{ (u_\ell, u_r) \in D : q_\ell, q_r \geq 0, \pi(\Gamma_{o,a_1}^-(u_\ell)) \cap \Gamma_{o,a_2}^+(u_r) \neq \emptyset \right\}, \quad (5.6)$$

where Γ_{o,a_1}^- and Γ_{o,a_2}^+ are defined in (2.14) and (2.15), respectively. In particular, if $(u_\ell, u_r) \in D_c$, then q_c^0 in (5.5) corresponds to the point of $\pi(\Gamma_{o,a_1}^-(u_\ell)) \cap \Gamma_{o,a_2}^+(u_r)$ with maximal flow.

Remark 5.2. If $a_1 = a_2$, then $\mathcal{RS}_c \equiv \mathcal{RS}_p$ by (5.5)₃ and Proposition 3.3. In this case π becomes the identity function and it is easy to prove that $\Gamma_{o,a_1}^-(u_\ell) \cap \Gamma_{o,a_2}^+(u_r)$ has at most one element; therefore $\mathfrak{Q}(u_\ell, u_r)$ contains at most one point, and hence the maximization procedure to compute q_c^0 in (5.4)₁ is not needed. This is why that procedure does not appear in Section 4.1.

On the other hand, if $a_1 \neq a_2$ then $\mathfrak{Q}(u_\ell, u_r)$ can contain infinitely many elements, see Figure 12.

We now prove that there exist $a_2 > a_1$ such that \mathcal{RS}_c is not coherent. Note that in the case $a_1 = a_2$ we can apply the results in Subsection 4.1 and deduce that, on the contrary, the c-Riemann solver is coherent.

Proposition 5.3. *There exist $a_2 > a_1$ such that the c-Riemann solver \mathcal{RS}_c corresponding to (5.5) is not coherent.*

Proof. For every (u_ℓ, u_r) in D_c , see (5.6), we have that $(u_c^-, u_c^+) \doteq C(u_\ell, u_r)$ belongs to D_c because $q_c^0 \geq 0$ and $u_c^+ \in \pi(\Gamma_{o,a_1}^-(u_c^-)) \cap \Gamma_{o,a_2}^+(u_c^+)$ since $(u_c^-, u_c^+) \in (\Gamma_{o,a_1}^-(u_c^-), \Gamma_{o,a_2}^+(u_c^+))$ and $u_c^+ = \pi(u_c^-)$. In particular this implies that $C(u_c^-, u_c^+)$ is well defined. Hence, to prove the statement we need to show the existence of $a_2 > a_1$ and $(u_\ell, u_r) \in D_c$ such that $C(u_c^-, u_c^+) \neq (u_c^-, u_c^+)$, see Figure 13. The main point is to choose (u_ℓ, u_r) in D_c so that $\pi(\bar{u}_{a_1}(u_\ell))$ lies on the lower boundary $B_{a_2}^+(u_r)$ of the set identified by (III) in Corollary 2.11, see Figure 7, hence $\pi(\bar{u}_{a_1}(u_\ell))$ does not belong to $\Gamma_{o,a_2}^+(u_r)$ defined in (2.15). On the other hand, by the construction detailed below, $\pi(\bar{u}_{a_1}(u_\ell)) = \pi(\bar{u}_{a_1}(u_c^-))$ does belong to $\Gamma_{o,a_2}^+(u_c^+)$.

As a first step, fix $u_r \in \Omega$ with $v(u_r) > a_2$. Let $u_\ell \in \Omega$ be the unique state with $q_\ell = 0$ and such that

$$0 < \tilde{q}_{a_2} \left(\pi(\bar{u}_{a_1}(u_\ell)), u_r \right) = \bar{q}_{a_1}(u_\ell) < q_{a_2}^a(u_r).$$

The above conditions express the fact that $\pi(\bar{u}_{a_1}(u_\ell))$ belongs to $B_{a_2}^+(u_r)$; hence $\pi(\bar{u}_{a_1}(u_\ell))$ does not belong to $\Gamma_{o,a_2}^+(u_r)$. The point $\pi(\bar{u}_{a_1}(u_\ell))$ is indeed the unique intersection of $B_{a_2}^+(u_r)$ with the image $q = a_2^2 \rho / a_1$ via π of the sonic line $q = a_1 \rho$ (note that $v(\bar{u}_{a_1}(u_\ell)) = a_1$).

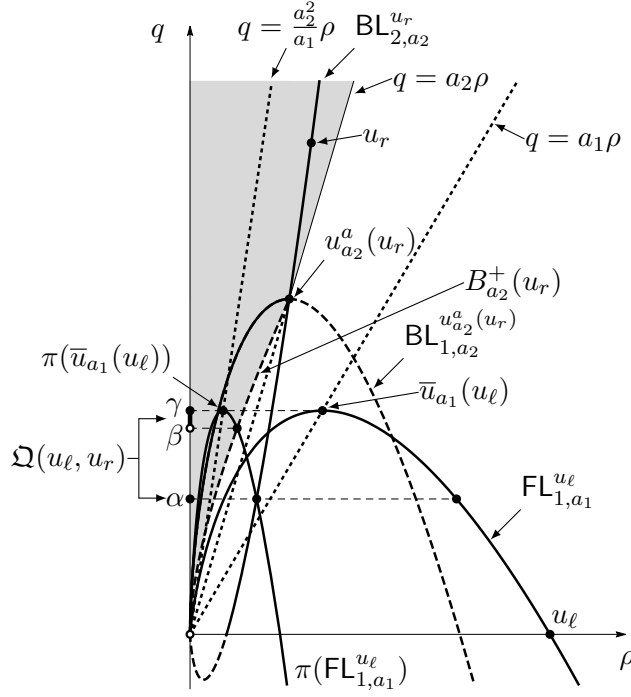


Figure 12: In the case represented above $\Omega(u_\ell, u_r) = \{\alpha\} \cup (\beta, \gamma]$ has infinitely many elements.

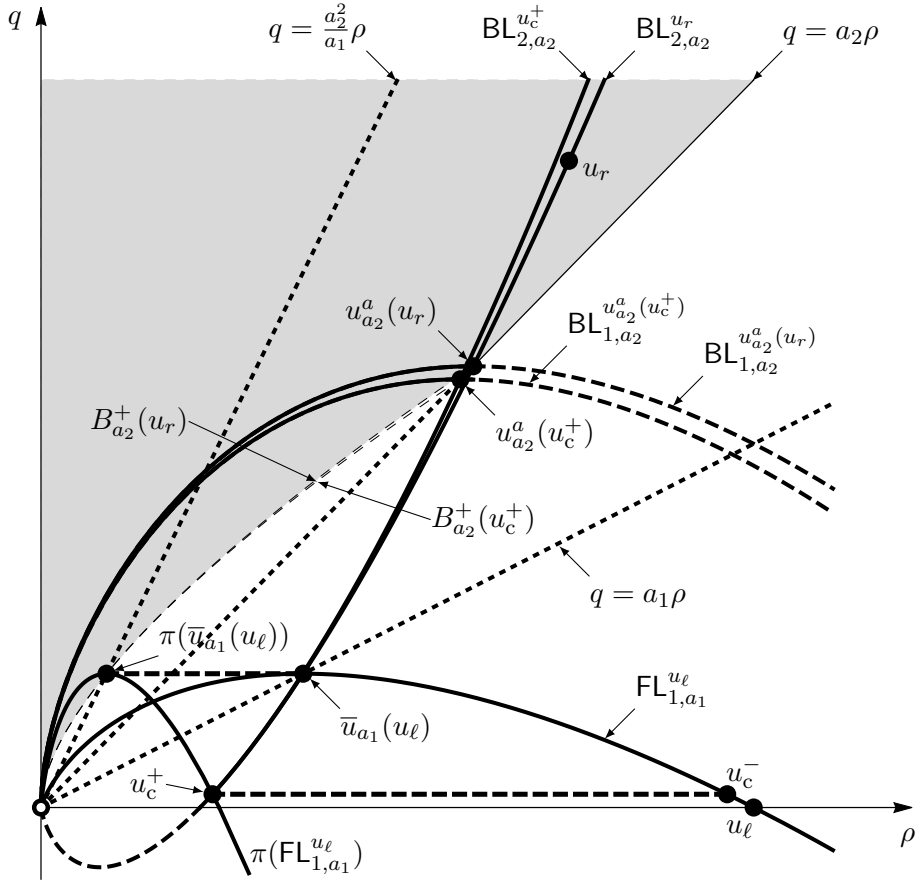


Figure 13: Construction given in the proof of Proposition 5.3. The shaded region and the solid black lines represent $\Gamma_{o,a_2}^+(u_r)$. Above $a_1 = 1$, $a_2 = 2$ and $u_r = (10, 24)$.

By Lemmas 2.10 and 2.11 we have $\pi(\Gamma_{o,a_1}^-(u_\ell)) \cap \Gamma_{o,a_2}^+(u_r)$ has at most one element. In fact, uniqueness is clear in the current construction; however, the existence is not granted, because the

intersection of $\pi(\text{FL}_{1,a_1}^{u_\ell})$ with $\text{BL}_{2,a_2}^{u_r}$ could have negative flow. Choose a_1, a_2 and u_r such that $\pi(\Gamma_{\alpha,a_1}^-(u_\ell)) \cap \Gamma_{\alpha,a_2}^+(u_r)$ has an element, which we denote by $u_c^+ = (\rho_c^+, q_c^0)$, with $q_c^0 > 0$; we provide a numerical evidence of the existence of such a choice in Figure 13. Then we have $C(u_\ell, u_r) = (u_c^-, u_c^+)$ with $u_c^- = \hat{u}_{a_1}(q_c^0, u_\ell) \neq u_\ell$ by (5.5). Recall that $(u_c^-, u_c^+) \in D_c$, as already observed at the beginning of the proof.

We claim that $C(u_c^-, u_c^+) \neq (u_c^-, u_c^+)$. Observe that $\mathcal{BL}_{2,a_2}^{u_c^+} > \mathcal{BL}_{2,a_2}^{u_r}$ in (ρ_c^+, ∞) , see item **(d)** in Lemma 2.1, hence $q_{a_2}^a(u_c^+) < q_{a_2}^a(u_r)$ because the sonic line $q = a_2\rho$ intersects first $\mathcal{BL}_{2,a_2}^{u_c^+}$ and then $\mathcal{BL}_{2,a_2}^{u_r}$. As a consequence, the boundary $B_{a_2}^+(u_c^+)$ lies below $B_{a_2}^+(u_r)$, and, in particular, $\pi(\bar{u}_{a_1}(u_c^-))$ belongs to $\Gamma_{\alpha,a_2}^+(\bar{u}_{a_1}(u_c^-))$. Let us stress that $\bar{u}_{a_1}(u_c^-) = \bar{u}_{a_1}(u_\ell)$ because $u_c^- \in R_{1,a_1}^{u_\ell}$ and therefore $\mathcal{R}_{1,a_1}^{u_\ell} \equiv \mathcal{R}_{1,a_1}^{u_c^-}$ in $(0, \rho_c^-]$ by item **(f)** in Lemma 2.1. These considerations imply that $C(u_c^-, u_c^+) = (\bar{u}_{a_1}(u_\ell), \pi(\bar{u}_{a_1}(u_\ell)))$, which differs from (u_c^-, u_c^+) . \square

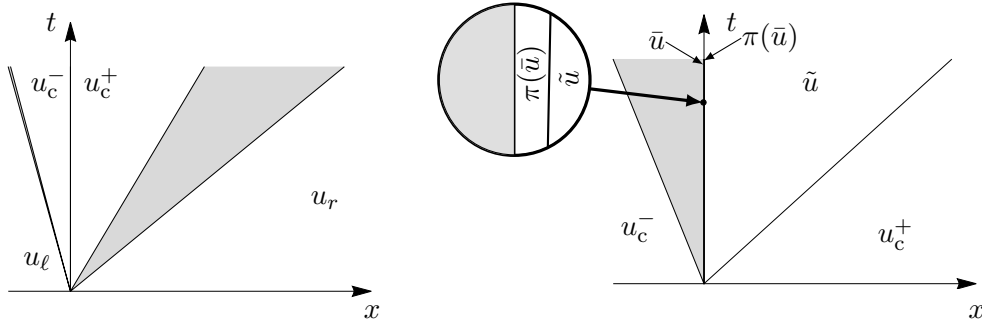


Figure 14: Two solutions constructed in Remark 5.4. Above we denoted $\bar{u}_{a_1}(u_\ell)$ by \bar{u} and $\tilde{u}_{a_2}(\pi(\bar{u}_{a_1}(u_\ell)), u_c^+)$ by \tilde{u} .

Remark 5.4. For a better understanding of the counterexample constructed in the above proof, we show how the two Riemann problems corresponding to (u_ℓ, u_r) and (u_c^-, u_c^+) are solved. The Riemann problem with initial datum (u_ℓ, u_r) is solved by a subsonic 1-rarefaction with negative speeds connecting u_ℓ to u_c^- , a stationary discontinuity from u_c^- to u_c^+ , and a 2-rarefaction from u_c^+ to u_r , whose tail is subsonic and its head is supersonic, see Figure 14 on the left. The Riemann problem with initial datum (u_c^-, u_c^+) is solved by a 1-rarefaction from u_c^- to $\bar{u}_{a_1}(u_\ell)$, whose left state is subsonic and its right state is sonic, and ends at $\xi = 0$, a stationary discontinuity from $\bar{u}_{a_1}(u_\ell)$ to $\pi(\bar{u}_{a_1}(u_\ell))$, an “almost stationary” 1-shock from $\pi(\bar{u}_{a_1}(u_\ell))$ to $\tilde{u}_{a_2}(\pi(\bar{u}_{a_1}(u_\ell)), u_c^+)$ and a 2-shock from $\tilde{u}_{a_2}(\pi(\bar{u}_{a_1}(u_\ell)), u_c^+)$ to u_c^+ , see Figure 14 on the right. In particular, the second solution does not coincide with the piecewise function

$$\xi \mapsto \begin{cases} u_c^- & \text{if } \xi < 0, \\ u_c^+ & \text{if } \xi \geq 0, \end{cases}$$

and this implies that (u_ℓ, u_r) belongs to the coherence domain CH of \mathcal{RS}_c .

We now illustrate by numerical examples the statement of Proposition 5.3. The construction given in the proof of that proposition with data $a_1 = 1$, $a_2 = 2$, $u_r = (10, 24)$ and the approximations in the computations, lead us to consider $u_\ell = (13.47, 0)$. Figures 15a and 15b show the correct solution, corresponding to $\mathcal{RS}_c[u_\ell, u_r]$, which is obtained when the traces u_c^\pm are computed *once and for all* at the initial time. Figures 15c and 15d presents the case where the traces are *updated at each time step*. The procedure of updating u_c^\pm at each time step, which is usual in numerical schemes for general initial-value problems, has the serious drawback of introducing nearby *incoherent* states. The solution obtained in this way substantially differs from the right one (see also Remark 5.4 and Figure 14): a small rarefaction wave on the left is missing, the jump at 0 is solved by a rarefaction instead of a shock wave, and the plateau following it is higher and much longer; moreover, oscillations appear in the plateau in the region $x > 0$. Observe that Figures 15a and 15b correspond to Figure 14 on the left; moreover, in a sense, the solution $u_\Delta(t, x)$ represented in Figures 15c and 15d at time $t = 0.2$ can be obtained for $t \in [0, 2\Delta t)$ by merging the solutions represented in Figure 14 on the left, at $t = 0$,

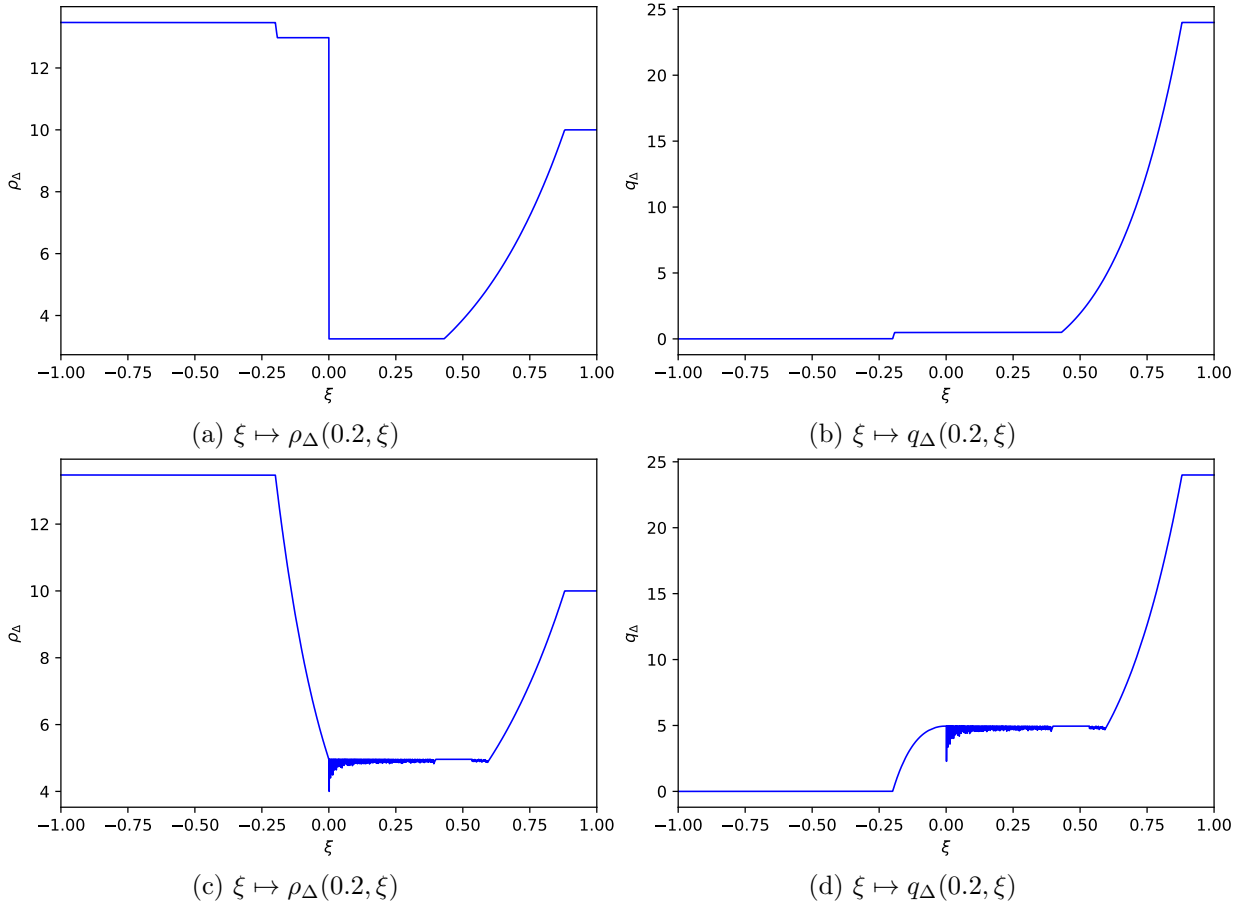


Figure 15: Numerical illustration of the incoherence of the c -Riemann solver corresponding to (5.5). Left column: the traces u_c^{\pm} are computed once and for all at the initial time. Right column: the traces are updated at each time step.

and on the right, at $t = \Delta t$. The above considerations demonstrate the instability of the scheme in this case, caused by the incoherence of \mathcal{RS}_c .

Proposition 5.5. *There exist $a_2 > a_1$ such that the c -Riemann solver corresponding to (5.5) is not $\mathbf{L}_{\text{loc}}^1$ -continuous with respect to the initial data.*

Proof. Let $(u_\ell, u_r) \in D_c$ be as in the proof of Proposition 5.3. Fix $\varepsilon > 0$ sufficiently small and define $u_\ell^\varepsilon \doteq (\rho_\ell + \varepsilon, 0)$. Observe that $\mathbf{FL}_{1,a_1}^{u_\ell^\varepsilon}$ lies above $\mathbf{FL}_{1,a_1}^{u_\ell}$, hence $\pi(\bar{u}_{a_1}(u_\ell^\varepsilon))$ belongs to $\Gamma_{o,a_2}^+(u_r)$. As a consequence $\mathcal{RS}_c[u_\ell^\varepsilon, u_r]$ has a 1-rarefaction with negative speeds connecting u_ℓ^ε and $\bar{u}_{a_1}(u_\ell^\varepsilon)$, a stationary discontinuity from $\bar{u}_{a_1}(u_\ell^\varepsilon)$ to $\pi(\bar{u}_{a_1}(u_\ell^\varepsilon))$, an “almost stationary” 1-shock from $\pi(\bar{u}_{a_1}(u_\ell^\varepsilon))$ to $\tilde{u}_{a_2}(\pi(\bar{u}_{a_1}(u_\ell^\varepsilon)), u_r)$ and a 2-rarefaction from $\tilde{u}_{a_2}(\pi(\bar{u}_{a_1}(u_\ell^\varepsilon)), u_r)$ to u_r . By letting ε tend to zero the speed of the 1-shock goes to zero and therefore $\mathcal{RS}_c[u_\ell^\varepsilon, u_r]$ converges in $\mathbf{L}_{\text{loc}}^1$ to

$$\begin{cases} \mathcal{RS}_{p,a_1}[u_\ell, \bar{u}_{a_1}(u_\ell)](\xi) & \text{if } \xi < 0, \\ \mathcal{RS}_{p,a_2}[\bar{u}_{a_1}(u_\ell), u_r](\xi) & \text{if } \xi \geq 0, \end{cases}$$

which differs from $\mathcal{RS}_c[u_\ell, u_r]$ constructed in Remark 5.4. □

We do not consider the case $a_1 > a_2$ not to overload the paper.

6 Compressors

In Sections 4 and 5 we investigated the well-posedness and coherence of several couplings at the intersection of two pipes. Such couplings are rather general, but they are understood to model “free” flows through the junction. From this section on, we focus instead on couplings where external forces, modeling the action of some device or friction effects, take place. We begin with compressors.

A compressor is powered by the gas flowing through it; however, the gas consumption is very low [40, p. 86] and is usually neglected in the modeling. To include the flux reduction due to gas consumption (but discarding the gas loss in the pipe) one replaces the first Rankine-Hugoniot condition (2.5) at $x = 0$, i.e., $q_c^- = q_c^+$, with $(1 - \bar{c})q_c^- = q_c^+$, where \bar{c} is the flux fraction used by the compressor [40, (17)]. We do not consider this case, which can be easily dealt as below by taking $\pi_2(\rho, q) = (1 - \bar{c})q$.

The purpose of a compressor is twofold. On the one hand, it increases the pressure and then the density of the gas, i.e., $p(\rho_c^-) < p(\rho_c^+)$ and $\rho_c^- < \rho_c^+$. On the other hand, it reduces the outlet velocity, i.e., $v(\rho_c^-) > v(\rho_c^+)$, because u_c^- and u_c^+ have the same flow q_c^0 but $\rho_c^- < \rho_c^+$. The latter feature facilitates the occurrence of subsonic states and reduces the possibility of potentially dangerous supersonic outflows.

The increase of the outflow pressure forces a higher outflow temperature; then, the isothermal pressure (2.3) should be replaced by an isentropic pressure. We assume that the temperature rise is negligible, as it is done in [24, (3), (59)], [34, (1.2), (1.5b)], [36, (7), (10b)], [40, (1), (15) and (16b)], and still consider (2.3). The isentropic case can be dealt as well with slightly heavy computations.

We consider below both two-way and one-way flows; the compressor is located at $x = 0$. In both two-way cases, we show that the coupling conditions do not select a unique coupling function C . On the contrary, in the one-way cases, we prove the uniqueness of C and the coherence of the corresponding c-Riemann solver.

6.1 Two-way flows

A first modeling assumes that the ratio between the incoming and outgoing pressures is constant. If the compressor is switched on, then this ratio is greater than one if the flow at $x = 0$ is positive, otherwise it is less than one; if the compressor is switched off then this ratio equals one. The corresponding coupling condition can be written as

$$p(\rho_c^+) = \left(1 + K_p(q_c^0)\right) p(\rho_c^-). \quad (6.1)$$

Here, if the compressor is switched on then either $K_p(q_c^0) > 0$ in the case $q_c^0 > 0$ or $K_p(q_c^0) \in (-1, 0)$ otherwise; if the compressor is switched off then $K_p(q_c^0) = 0$, see [27, (9)]. Observe that if $K_p(q_c^0) = 0$ then condition (6.1) reduces to (4.1), which has already been studied in Subsection 4.1. For this reason, below we assume that the compressor is always switched on, i.e., $K_p(q_c^0) \neq 0$.

In general K_p depends on time; we assume K_p to be piecewise constant since we are interested in the corresponding c-Riemann solver. More precisely, we focus on

$$K_p(q_c^0) = \begin{cases} K_p^- & \text{if } q_c^0 \leq 0, \\ K_p^+ & \text{if } q_c^0 > 0, \end{cases} \quad -1 < K_p^- < 0 < K_p^+. \quad (6.2)$$

Note that (6.1) corresponds to $\pi: \Omega \rightarrow \Omega$ defined by (see Theorem 3.8)

$$\pi(\rho, q) \doteq \left((1 + K_p(q)) \rho, q \right).$$

Notice that the model seems not to be completely meaningful when $q_c^0 = 0$. However, the counterexample showed in the proof of the next proposition avoids null flows at $x = 0$. Also notice that the counterexample only involves subsonic flows.

Proposition 6.1. *Fix $K_p^-, K_p^+ \in \mathbb{R}$ such that $-1 < K_p^- < 0 < K_p^+$. Condition (6.1) does not select a unique c-Riemann solver in \mathbf{D} .*

Proof. It is sufficient to fix $u_\ell, u_r \in \Omega$ with $\rho_r \geq \underline{\rho}(u_r)$ and such that there exist $u_1^-, u_2^- \in \text{FL}_1^{u_\ell}$ with $q_1^- > 0 > q_2^-$, $\pi_1(u_2^-) \geq \underline{\rho}(u_r)$ and such that $\pi(u_1^-), \pi(u_2^-) \in \text{BL}_2^{u_r}$, see for instance Figure 16. Note that by (6.2) we have $\rho_1^+ = (1 + K_p^+)\rho_1^-$ and $\rho_2^+ = (1 + K_p^-)\rho_2^-$. \square

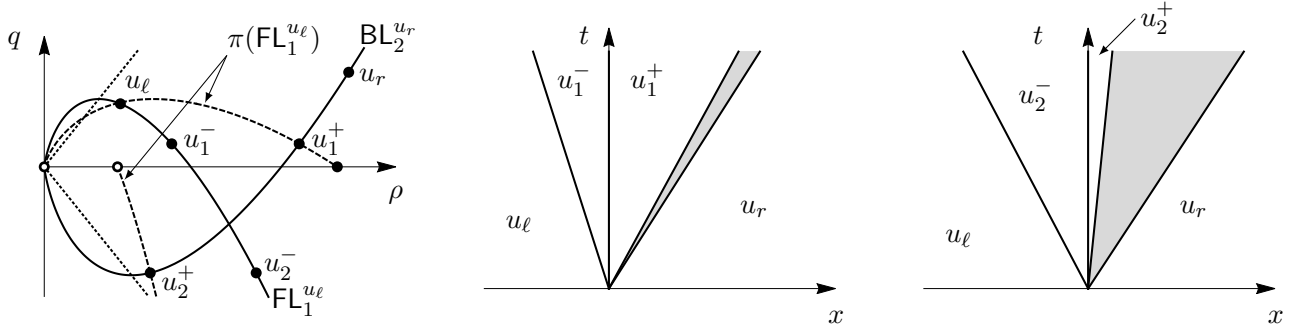


Figure 16: Two solutions satisfying the coupling condition (6.1). With a slight abuse of notation, we use u_1^\pm and u_2^\pm in place of u_c^\pm and corresponding to the two solutions.

A different modeling considers the coupling condition

$$|q_c^0| \left(\left(p(\rho_c^+) / p(\rho_c^-) \right)^{\text{sign}(q_c^0) \kappa} - 1 \right) = K, \quad (6.3)$$

at $x = 0$, where $\kappa \in [2/7, 2/5]$ is a parameter that depends on the gas under consideration and $K \geq 0$ is the compressor power, see [32, (18) and first line on page 2106].

Assume the compressor is switched off, i.e., $K = 0$. Then either $p(\rho_c^+) = p(\rho_c^-)$ or $q_c^0 = 0$, while in the previous case (6.1)-(6.2) only the former possibility occurred. If $p(\rho_c^+) = p(\rho_c^-)$, then condition (6.3) reduces to (4.1), which is dealt as in Subsection 4.1. If $q_c^0 = 0$, then the corresponding c-Riemann solver does not coincide with \mathcal{RS}_p on D_c and then the compressor influences the flow across $x = 0$ even if it is switched off.

Proposition 6.2. *Fix $K \geq 0$. Condition (6.3) does not select a unique c-Riemann solver in D .*

Proof. Assume $K = 0$. Let $u_\ell, u_r \in \Omega$ be such that $u_p^- = u_p^+$ and take $u_c^- = \hat{u}(0, u_\ell)$, $u_c^+ = \check{u}(0, u_r)$. Then both u_p and u_c satisfy (6.3) but they differ.

If $K > 0$, we can proceed as in the proof of Proposition 6.1 and show that (6.3) does not yet select a unique c-Riemann solver. Indeed, in this case $q_c^0 \neq 0$ and (6.3) is equivalent to

$$p(\rho_c^+) = \left(1 + \frac{K}{|q_c^0|} \right)^{\text{sign}(q_c^0) / \kappa} p(\rho_c^-),$$

which is analogous to (6.1). □

6.2 One-way flows

Consider the coupling condition (6.1)-(6.2), and assume that the flow is one-way, say $q \geq 0$. Then the corresponding coupling condition writes

$$p(\rho_c^+) = (1 + K_p^+) p(\rho_c^-), \quad (6.4)$$

for a constant $K_p^+ > 0$, see [38, (4)] and [46, (20)₂]. Condition (6.4) implies $u_c^+ = \pi(u_c^-)$, where $\pi \doteq (\pi_1, \pi_2): \Omega \rightarrow \Omega$ is defined by

$$\pi(\rho, q) \doteq \left((1 + K_p^+) \rho, q \right). \quad (6.5)$$

In Figure 17 we represent $\pi(\text{FL}_1^{u_\ell})$ for a fixed subsonic state $u_\ell \in \Omega$ with $q_\ell > 0$.

Note that $\pi(u)$ lies on the right of u for any $u \in \Omega$; moreover, if $u_1, u_2 \in \Omega$ are respectively supersonic and subsonic states, then $\pi(u_1)$ lies on the left of $\pi(u_2)$. Observe that

$$D_c = \left\{ (u_\ell, u_r) \in D : q_\ell, q_r \geq 0, \pi(\Gamma_\circ^-(u_\ell)) \cap \Gamma_\circ^+(u_r) \neq \emptyset \right\}, \quad (6.6)$$

where Γ_\circ^- and Γ_\circ^+ are defined in (2.14) and (2.15), respectively. Then, for every $(u_\ell, u_r) \in D_c$, we have $v(u_c) \geq 0$ in the whole of \mathbb{R} by (2.14) and (2.15), see also Corollaries 2.10 and 2.11.

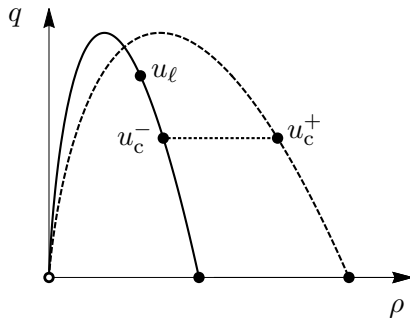


Figure 17: Portion of $\text{FL}_1^{u_\ell}$ with non-negative flux, solid line, and its image through π defined in (6.5), dashed line. Here, $K_p^+ = 1$.

Proposition 6.3. Fix $K_p^+ > 0$. If the flow is one-way with $q \geq 0$, then the coupling condition (6.4) selects a unique coupling function C in the set D_c given in (6.6). Moreover, the c -Riemann solver \mathcal{RS}_c corresponding to (6.4) is coherent.

Proof. First, we prove that C is well defined in D_c . This is equivalent to show that for any (u_ℓ, u_r) in D_c there exists a unique pair (u_c^-, u_c^+) in $\Gamma_o^-(u_\ell) \times \Gamma_o^+(u_r)$ such that $u_c^+ = \pi(u_c^-)$. By (6.6) we have the existence of such a pair; we prove now that it is unique. Notice that (6.4) implies (3.6); therefore, there are only two possible ways to construct a c -solution, that correspond to **(1)** and **(2)** in Corollary 3.6. Observe that $\text{BL}_2^{u_r} \cap \pi(\Gamma_o^-(u_\ell))$ has at most one element, see Figures 1, 6 and 17; hence, there exists at most one $u^- \in \Gamma_o^-(u_\ell)$ such that $\pi(u^-) \in \text{BL}_2^{u_r}$. Then, referring to that corollary, the unique candidates for u_c^- are u_ℓ in case **(1)** and u^- in case **(2)**. We need to show now that it is possible to construct a c -solution satisfying **(1)** if and only if it is not possible to construct a c -solution satisfying **(2)**. This is equivalent to show that u_ℓ is supersonic and $\pi(u_\ell) \in \Gamma_o^+(u_r)$ if and only if $\text{BL}_2^{u_r} \cap \pi(\Gamma_o^-(u_\ell)) = \emptyset$.

Assume by contradiction, see Figure 18, that there exists $(u_\ell, u_r) \in D_c$ with both u_ℓ supersonic (hence $q_\ell > 0$), $\pi(u_\ell) \in \Gamma_o^+(u_r)$, and $u^- \in \Gamma_o^-(u_\ell)$, which is non-supersonic with $q^- > 0$, $\pi(u^-) \in \text{BL}_2^{u_r}$. Note that $v(u^-) \leq a < v(u_\ell)$; hence $u^- \neq u_\ell$. By **(I)** in Corollary 2.10 we deduce that $\mathcal{RS}_p[u_\ell, u^-]$ only consists of a 1-shock, hence $q_\ell > q^-$ and $\rho_\ell < \rho^-$. As a consequence, see Figure 17, we have $\pi_1(u_\ell) < \pi_1(u^-)$ and $\pi_2(u_\ell) = q_\ell > q^- = \pi_2(u^-)$. These considerations and the fact that $\pi(u^-) \in \text{BL}_2^{u_r}$ imply that $\pi(u_\ell)$ cannot belong to $\text{BL}_2^{u_r}$ but lies on its left, because $\text{BL}_2^{u_r}$ is strictly increasing in $q \geq 0$. Hence $\mathcal{RS}_p[\pi(u_\ell), u_r]$ involves a 1-shock, which has positive propagation speed because $\pi(u_\ell) \in \Gamma_o^+(u_r)$; therefore $\pi(u_\ell)$ is non-subsonic by (b) in Proposition 2.7. As a consequence,

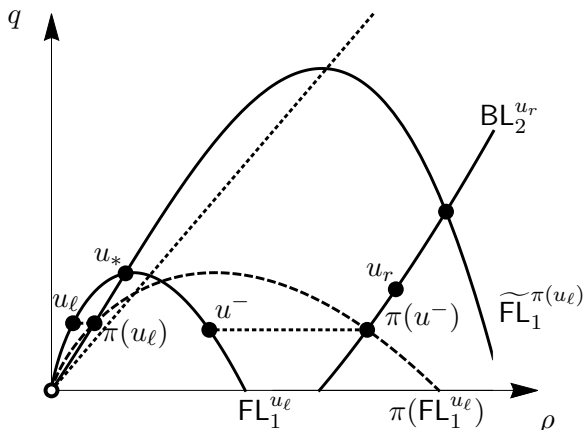


Figure 18: A hypothetical configuration where both cases **(1)** and **(2)** of Corollary 3.6 occur simultaneously. Above, $\widetilde{\text{FL}}_1^{\pi(u_\ell)}$ represents a “fake” $\text{FL}_1^{\pi(u_\ell)}$; in fact, in the proof of Proposition 6.3 we show that this configuration cannot occur.

there exists $u_* \in \text{FL}_1^{u_\ell} \cap \text{FL}_1^{\pi(u_\ell)}$ with $\rho_\ell < \pi_1(u_\ell) < \rho_*$ and $\pi_2(u_\ell) = q_\ell < q_*$, see Figure 18; hence $u_* \in \text{S}_1^{u_\ell} \cap \text{S}_1^{\pi(u_\ell)}$ and therefore $u_\ell, \pi(u_\ell) \in \text{S}_1^{u_*}$ by **(f)** in Lemma 2.1. This leads to a contradiction:

by the concavity of $\mathcal{S}_1^{u_*}$, see item **(c)** in Lemma 2.1, the intersection $\mathcal{S}_1^{u_*} \cap \{(\rho, q_\ell) : \rho \in (0, \rho_*)\}$ has at most one element because $q_\ell < q_*$. This proves our claim. Then, the coupling function C is well defined.

Second, we show that the c -Riemann solver is coherent. We proved above that the coupling function C associated to (6.4) is well defined in D_c . Fix $(u_\ell, u_r) \in D_c$ and consider $(u_c^-, u_c^+) = C(u_\ell, u_r)$. We have $(u_c^-, u_c^+) \in \Gamma_o^-(u_\ell) \times \Gamma_o^+(u_r)$ and $u_c^+ = \pi(u_c^-)$; moreover, $(u_c^-, u_c^+) \in \Gamma_o^-(u_c^-) \times \Gamma_o^+(u_c^+)$ and therefore $u_c^+ = \pi(u_c^-) \in \pi(\Gamma_o^-(u_c^-)) \cap \Gamma_o^+(u_c^+) \neq \emptyset$. Hence $(u_c^-, u_c^+) \in D_c$ and then **(1)** in Theorem 3.8 holds.

We now prove **(2)** in Theorem 3.8. Fix $(u^-, u^+) \in D_c$. If $(u^-, u^+) = C(u_\ell, u_r)$, then $(u^-, u^+) \in \Gamma_o^-(u_\ell) \times \Gamma_o^+(u_r)$ by (3.3) and $u^+ = \pi(u^-)$ by (6.4) and (6.5). Conversely, if $(u^-, u^+) \in \Gamma_o^-(u_\ell) \times \Gamma_o^+(u_r)$ and $u^+ = \pi(u^-)$ then $(u^-, u^+) = (u_c^-, u_c^+) = C(u_\ell, u_r)$ by the uniqueness showed above. Thus also **(2)** in Theorem 3.8 holds.

Item **(3)** in Theorem 3.8 holds by the uniqueness showed above. Therefore Theorem 3.8 applies and this concludes the proof. \square

As already observed in the first part of the above proof, (6.4) implies (3.6); hence, the structure of the solution is as described in Corollary 3.6.

Remark 6.4. The flow can be supersonic across the compressor, i.e., $v(u_c^-), v(u_c^+) > a$. Indeed, according to the last statement in Corollary 3.6, we have $v(u_c^-) > a$ if and only if both $u_c^- = u_\ell$ and $v(u_\ell) > a$; moreover, in this case we may also have $v(u_c^+) > a$, because $u_c^+ = \pi(u_c^-)$ and (6.5) imply $v(u_c^+) = q_c^0/\rho_c^+ \approx v(u_c^-) = q_c^0/\rho_c^-$ for K_p^+ sufficiently small.

Now, consider the coupling condition (6.3). Assume that the flow is one-way, say $q \geq 0$, and that the compressor is switched on, i.e., $K > 0$. Then the corresponding coupling condition can be written as

$$q_c^0 \left(\left(p(\rho_c^+)/p(\rho_c^-) \right)^\kappa - 1 \right) = K, \quad (6.7)$$

see [12, (3.1.39), (3.1.40), (3.1.41)], [24, (59)], [34, (1.5b)], [36, (10b)], [40, (15) and (16b)], [41, (C3)], [52, § 2.3], [53, (71) and (74)]. In [24] and [34] the authors let κ vary in $[2/7, 2/5]$ and $[1/3, 3/5]$, respectively. By the assumptions we have

$$\rho_c^+ > \rho_c^-, \quad q_c^0 > 0. \quad (6.8)$$

Therefore (6.7) is equivalent to

$$p(\rho_c^+) = \left(1 + \frac{K}{q_c^0} \right)^{1/\kappa} p(\rho_c^-).$$

Note that $u_c^+ = \pi(u_c^-)$, where $\pi \doteq (\pi_1, \pi_2) : \{(\rho, q) \in \Omega : q \neq 0\} \rightarrow \{(\rho, q) \in \Omega : q \neq 0\}$ is defined by

$$\pi(\rho, q) \doteq \left(\left(1 + \frac{K}{q} \right)^{1/\kappa} \rho, q \right). \quad (6.9)$$

In Figure 19 we represent $\pi(\text{FL}_1^{u_\ell})$ for a fixed subsonic state $u_\ell \in \Omega$ with $q_\ell > 0$. Note that $\pi(u)$ lies on the right of u for any $u \in \Omega$; moreover, if $u_1, u_2 \in \Omega$ are supersonic and subsonic states with $q_1 = q_2$, respectively, then $\pi(u_1)$ lies on the left of $\pi(u_2)$.

Observe that

$$D_c = \left\{ (u_\ell, u_r) \in D : q_\ell, q_r \geq 0, \pi(\Gamma_o^-(u_\ell)) \cap \Gamma_o^+(u_r) \neq \emptyset \right\}. \quad (6.10)$$

This implies $v(u_c) \geq 0$ in the whole of \mathbb{R} , for any $(u_\ell, u_r) \in D_c$, by (2.14) and (2.15), see also Corollaries 2.10 and 2.11.

The proof of the following proposition is analogous to that of Proposition 6.3 (it is sufficient to consider Figures 19, 20 in place of Figures 17, 18, respectively), and is then omitted.

Proposition 6.5. *Fix $K > 0$. If the flow is one-way with $q \geq 0$, then the coupling condition (6.7) selects a unique coupling function in the set D_c given in (6.10), and the corresponding c -Riemann solver is coherent.*

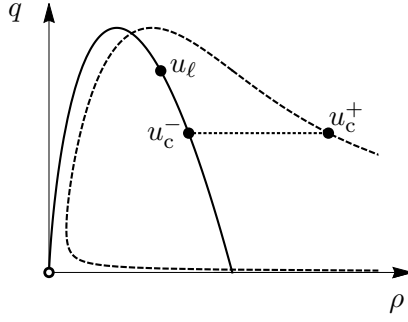


Figure 19: Portion of $FL_1^{u_\ell}$ with positive flux, solid line, and its image through π defined in (6.9), dashed line. Here, $K = 1/5$ and $\kappa = 11/30$.

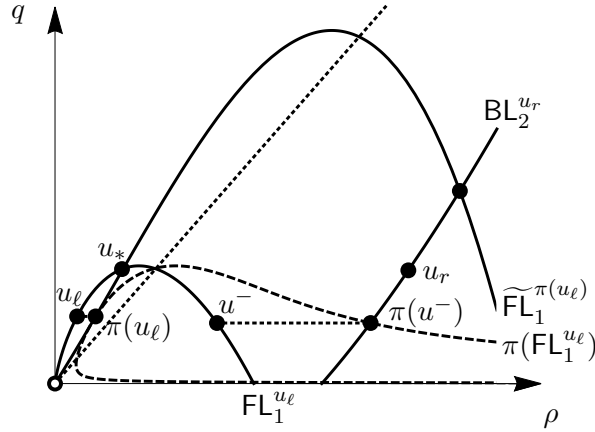


Figure 20: A hypothetical configuration where both cases **(1)** and **(2)** of Corollary 3.6 occur simultaneously. Above, $\widetilde{FL}_1^{\pi(u_\ell)}$ represents a “fake” $FL_1^{\pi(u_\ell)}$; in fact, it is possible to show that this configuration cannot occur.

Note that $(6.8)_1$ implies (3.6); hence the structure of the solution is as described in Corollary 3.6. A remark analogous to Remark 6.4 also holds in this case.

We conclude this subsection by mentioning the one-way flow through a compressor modeled in [37, § 2.3]; the modeling is as follows. If the compressor is active, then it increases the outflow pressure by an additive term $\Delta(t)$; if the compressor is in bypass mode, then the in- and outflow pressures are equal; the flow is zero if the compressor is closed. This simplified modeling is analogous to the one presented in Subsection 7.2 for valves (and then suffers in principle of the same drawbacks), with an important difference: while the action of a valve can be modeled as instantaneous, it takes time to compress the gas, and this is why $\Delta(t)$ depends on t . As a consequence, even if we prescribe the pressure rise to equal some constant $\bar{\Delta}$, to achieve this value it takes a time \bar{t} such that $\Delta(\bar{t}) = \bar{\Delta}$. As a consequence, this modeling falls out of our modeling (see however the similar “delayed” valve in [21, § 6]).

7 Valves

As well as compressors, valves are an important ingredient in gas networks. In this section we first briefly recall some recent results concerning their coherence and its physical meaning. Then we show that some simplified models usually exploited for flow optimizations in networks are not coherent.

7.1 Coherence and chattering

In this subsection we briefly resume the results contained in [19–22]. To the best of our knowledge, they are the first rigorous results about non-stationary isothermal flows through valves.

Pressure-relief valves are considered in [19]. A detailed study is done for case of a valve which is

closed if $|p(\hat{\rho}(0, u_r)) - p(\hat{\rho}(0, u_\ell))| \leq M$, for a fixed $M > 0$, otherwise it is open. The velocities of the flows are general: no assumption of subsonicity is done. In such a case, the coherence domain of the c-Riemann solver is explicitly provided. Other properties are studied as well: consistence, the $\mathbf{L}_{\text{loc}}^1$ -continuity domain of the solver, and examples of invariant domains. The lack of coherence has been interpreted in that paper as modeling the phenomenon of *chattering*, the rapid and repeated opening and closing of the valve; see [19–22] and references therein for more information on this phenomenon.

The case of one-way valves is discussed in [21]; this means that the flow through the valve is possible in a single direction. As an example of the general framework treated there, it was considered the case of a valve that aims at keeping a fixed outgoing flow $q_* > 0$; when this is not possible, then the valve shuts. Such valves are known as *pressure independent characterized control valves*. The main results are an explicit characterization of the coherence domain of the c-Riemann solver, and a discussion of the invariant domains. Also the case of a valve with a non-zero reaction time is considered.

The paper [22] deals with flux-maximizing valves. Moreover, the flow is imposed to occur within prescribed bounds of pressure and flow; this requirement clearly corresponds to the existence of invariant domains. Within this framework, three kinds of valves are described, which differ for their action; two of them lead to a coherent solver, the third one does not.

How to “remove” the chattering of valve? A theoretical answer to this issue is given in [20]: one has to modify the corresponding c-Riemann solver in order that it becomes coherent. An example of this procedure is shown for the (incoherent) c-Riemann solver considered in [21]; the new solver differs from the old one only for the states that led the old solver to lose coherence. Moreover, for incoherent initial data, the new solver selects the unique solution that maximizes the flow through the valve among all c-Riemann solvers. Several numerical simulations are also provided.

A partial conclusion of the results of the above papers is that the mechanism that leads to the loss of coherence, and then possibly trigger chattering, is hard to understand. Indeed, such a behavior strongly depends on the type of valve under consideration and establishing general criteria is not yet clear.

7.2 Control valves in optimization

An important issue in gas networks concerns the optimization of flows, depending on the presence of compressors, valves and other devices in the network [37,53]. The complexity of the problem essentially requires that the flows are constant in each pipe and variations only occur at the junctions. In this short subsection we briefly comment on how valves are modeled in such a framework and show such oversimplified modelings are not coherent.

A *control valve* can be modeled by the coupling conditions

$$\begin{aligned} p(\rho_c^+) &= p(\rho_c^-) - \Delta && \text{if the valve is active,} \\ p(\rho_c^+) &= p(\rho_c^-) && \text{if the valve is in bypass mode,} \\ q_c^0 &= 0 && \text{if the valve is closed,} \end{aligned}$$

where $\Delta > 0$, see [37, § 2.2] and [53, § 3.4.17]. In general the pressure difference Δ depends on time; we assume that it is constant since we are interested in the corresponding c-Riemann solver.

In the case the control valve is in bypass mode the comments in Subsection 4.1 apply and then $\mathcal{RS}_c \equiv \mathcal{RS}_p$. The case of a closed control valve corresponds to take $q_c^0 = 0$, $u_c^- = \hat{u}(0, u_\ell)$ and $u_c^+ = \check{u}(0, u_r)$; observe that $\hat{u}(0, u_\ell)$ and $\check{u}(0, u_r)$ are well defined for any $(u_\ell, u_r) \in \mathbf{D}$ because $0 \in (\underline{Q}(u_r), \overline{Q}(u_\ell))$ by (2.17). If the valve is always active, then the situation is more delicate. Indeed, the coupling condition

$$p(\rho_c^+) = p(\rho_c^-) - \Delta \tag{7.1}$$

has two main drawbacks: it neither selects a unique c-Riemann solver nor it is coherent, as we show in the next two propositions. For $\delta \doteq \Delta/a^2$ we first introduce $\pi: \Omega \rightarrow \Omega$ by $\pi(\rho, q) \doteq (\rho - \delta, q)$.

Proposition 7.1. *The coupling condition (7.1) does not select a unique c-Riemann solver.*

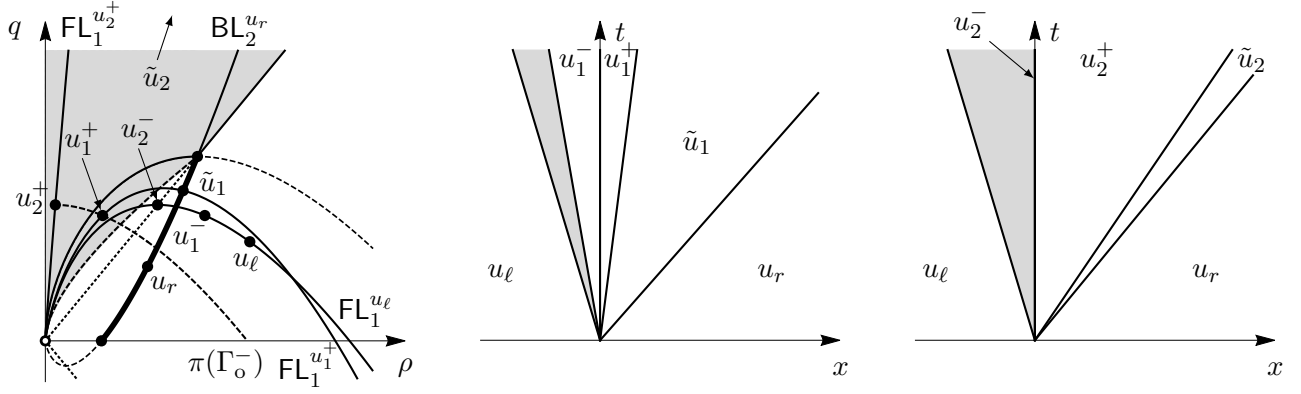


Figure 21: Two solutions satisfying the coupling condition (7.1). With a slight abuse of notation, we write u_1^\pm and u_2^\pm in place of u_c^\pm and corresponding to the two solutions. Moreover, we write $\pi(\Gamma_o^-)$ in place of $\pi(\Gamma_o^-(u_\ell))$ and \tilde{u}_i in place of $\tilde{u}_i(u_i^+, u_r)$, $i \in \{1, 2\}$. The solution on the right maximizes the flow across $x = 0$. The state \tilde{u}_2 is not represented in the figure on the left because its flux is too large.

Proof. For any $\Delta > 0$, it is easy to find $u_\ell, u_r \in \Omega$ such that $\pi(\Gamma_o^-(u_\ell)) \cap \Gamma_o^+(u_r)$ has more than one element, indeed infinitely many, see Figure 21. Then it is sufficient to observe that we can associate to any $u_c^+ \in \pi(\Gamma_o^-(u_\ell)) \cap \Gamma_o^+(u_r)$ a weak solution of the form (3.2) satisfying (7.1). \square

A simple way to fix the drawback pointed out in the above proposition consists in imposing a maximization property of the flow across the coupling: among all the c-Riemann solvers satisfying (7.1), we choose the one that maximizes the flow across $x = 0$. Such a c-Riemann solver is unique by the strict monotonicity of $\Gamma_o^-(u_\ell)$, but it is not coherent.

Proposition 7.2. *The c-Riemann solver satisfying (7.1) and maximizing the flow at $x = 0$ is not coherent.*

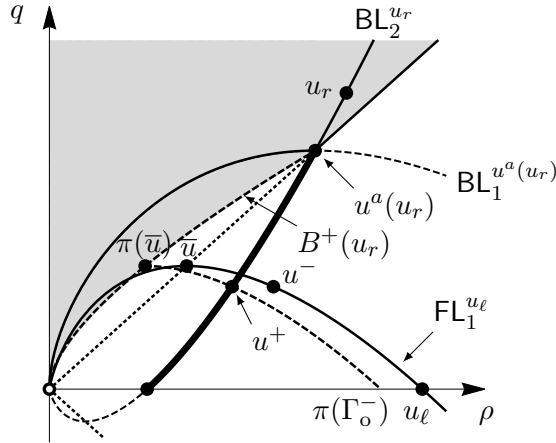


Figure 22: Construction given in the proof of Proposition 7.2. The shaded region and the solid thick black lines represent $\Gamma_o^+(u_r)$; its lower bound $B^+(u_r)$ is the dashed black line. We denote $\pi(\Gamma_o^-(u_\ell))$ by $\pi(\Gamma_o^-)$ and $\bar{u}(u_\ell)$ by \bar{u} .

Proof. For any $\Delta > 0$, it is easy to find $u_\ell, u_r \in \Omega$ with $v(u_r) > a$ and $q_\ell = 0$, such that $\pi(\bar{u}(u_\ell))$ belongs to $B^+(u_r)$, see Figure 22, and such that there exist $u^- \in \Gamma_o^-(u_\ell)$ and $u^+ \in \text{BL}_2^{u_r}$ satisfying $u^+ = \pi(u^-)$ and $0 < v(u^+) < a$. By construction we have $C(u_\ell, u_r) = (u^-, u^+)$. On the other hand, by reasoning as in the proof of Proposition 5.3, we deduce $C(u^-, u^+) = (\bar{u}(u_\ell), \pi(\bar{u}(u_\ell))) \neq (u^-, u^+)$ and this concludes the proof. \square

In [53, § 3.4.18] the authors consider a *control valve without remote access*. Such a valve is designed to keep the outgoing pressure below a given threshold, $p(\rho_c^+) \leq p^{\text{set}}$. The valve is in bypass mode

if $p(\rho_c^-) \leq p^{\text{set}}$, it automatically closes when $p(\rho_c^-) > p^{\text{set}} + \Delta$, where Δ is a constant; otherwise the control valve is active, reducing the pressure by some amount $\delta = \delta(u_\ell, u_r) \in (0, \Delta]$ so that $p(\rho_c^+) = p(\rho_c^-) - \delta = p^{\text{set}}$. As a result we have

$$p(\rho_c^+) = p(\rho_c^-) \quad \text{if } p(\rho_c^-) \leq p^{\text{set}}, \quad (7.2a)$$

$$p(\rho_c^+) = p^{\text{set}} \quad \text{if } p^{\text{set}} < p(\rho_c^-) \leq p^{\text{set}} + \Delta, \quad (7.2b)$$

$$q_c^0 = 0 \quad \text{if } p(\rho_c^-) > p^{\text{set}} + \Delta. \quad (7.2c)$$

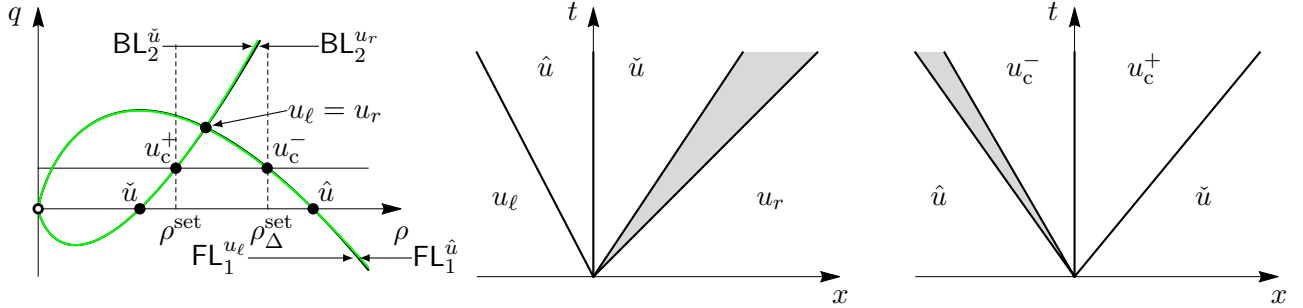


Figure 23: Incoherent Riemann data for the coupling conditions (7.2), see Proposition 7.3, with $u_\ell = u_r = (2, 1)$, $p^{\text{set}} \approx 1.64273$, $\Delta \approx 1.0968$ and $q_c^0(\hat{u}(0, u_\ell), \check{u}(0, u_r)) = 0.5$. Above we denoted p^{set}/a^2 by ρ^{set} , $(p^{\text{set}} + \Delta)/a^2$ by ρ_Δ^{set} , $\hat{u}(0, u_\ell) = u_c^-(u_\ell, u_r)$ by \hat{u} , $\check{u}(0, u_r) = u_c^+(u_\ell, u_r)$ by \check{u} , $u_c^-(\hat{u}(0, u_\ell), \check{u}(0, u_r))$ by u_c^- , $u_c^+(\hat{u}(0, u_\ell), \check{u}(0, u_r))$ by u_c^+ ,

Proposition 7.3. *The c-Riemann solver corresponding to a control valve without remote access corresponding to (7.2) is uniquely determined but not coherent.*

Proof. The proof is analogous to that of Proposition 7.2 (see also above it) and is therefore omitted, see Figure 23. The mutual positions of the (almost coinciding) curves $\text{BL}_2^{u_r}$ and $\text{BL}_2^{\check{u}}$ (as well as $\text{FL}_1^{u_\ell}$ and $\text{FL}_1^{\hat{u}}$) can be deduced by Lemma 2.1. \square

8 Resistors

Resistors are fictitious elements introduced to model the cumulative resistance of equipment (e.g., internal piping, filters), which cause a pressure loss at the intersection of the pipes in the direction of the flow. As a consequence, the momentum is not conserved at those points. The pressure drop $f_{\text{ext}} > 0$, which is not given analytically but provided by tables [25], depends on the geometry of the intersection, a resistance coefficient, the actual flow, and the pressure at the intersection.

As a first example, consider a one-way flow $q \geq 0$, with pressure laws $p_1(\rho) = a_1^2 \rho$ and $p_2(\rho) = a_2^2 \rho$ in the two pipes $x < 0$ and $x > 0$ as in Section 5, and assume that the pressure loss at the intersection is given by a constant quantity f_{ext} . Then we consider the coupling condition [2, (32)]

$$a_2^2 \rho_c^+ = a_1^2 \rho_c^- - f_{\text{ext}}. \quad (8.1)$$

If $a_1, a_2 > 0$ (possibly $a_1 = a_2$), then the c-Riemann solver associated to (8.1) is *not uniquely defined*; however, the c-Riemann solver associated to (8.1) and maximizing the flow at $x = 0$ is uniquely defined but it is *not coherent*. Indeed, it is easy to adapt the proofs of Propositions 7.1 and 7.2 by modifying the definition of π as $\pi(\rho, q) \doteq \left(\frac{a_1^2}{a_2^2} \rho - \frac{f_{\text{ext}}}{a_2^2}, q \right)$.

As a further example, assume the absolute pressure loss is either constant [53, (12)]

$$p(\rho_c^+) = p(\rho_c^-) - \text{sign}(q_c^0) \Delta, \quad (8.2)$$

or modeled by a quadratic function of the (turbulent) flow [53, (13)]

$$p(\rho_c^+) = p(\rho_c^-) - K_p \frac{|q_c^0| q_c^0}{\rho_c^-}. \quad (8.3)$$

Condition (8.2) coincides with (7.1) in the case $q_c^0 \geq 0$. Then, it is clear that (8.2) does not select a unique c-Riemann solver, see Proposition 7.1; uniqueness occurs if the flow is one-way and by imposing the flow maximization property at the coupling, but in this case the c-Riemann solver is not coherent, see Proposition 7.2.

We turn now to (8.3). Observe that $u_c^+ = \pi(u_c^-)$, where $\pi: \Omega \rightarrow \Omega$ is defined for $\kappa_p \doteq K_p/a^2$ by $\pi(\rho, q) \doteq (\rho - \kappa_p |q| q / \rho, q)$. Also (8.3) does *not* select a unique c-Riemann solver (by reasoning as in Proposition 7.1). However, if we impose a maximization property of the flow across the coupling, then it selects a *unique* c-Riemann solver; nevertheless, it is not coherent (by arguing as in Proposition 7.2).

9 Conclusions and some open problems

In this paper we provided a general framework for the study of coupling Riemann problems and provided some results about their coherence. This mathematical problem arises in the modeling of gas flows through two connected pipes. Rather surprisingly, some coupling conditions proposed in the literature do not give rise to a unique coupling Riemann solver; other conditions have instead this property but the corresponding solver fails to be coherent. At last, there still are some conditions satisfying both requirements. For the reader's convenience, we provide an overview of our results in Table 1.

Our analysis is restricted for simplicity to the isothermal Euler system, but it could be generalized to several extents. For instance, to isentropic flows and to general flows modeled by the full 3×3 Euler system. For brevity, we did not address explicitly the case of pipes with different cross-sectional areas [16–18], or misaligned [16, 17]; also these cases could be dealt following the lines above. Analogously, it is not hard to extend to two-way flows what we discussed of the one-way flows only.

There are however several related problems that would deserve consideration but to which this paper does not provide answers. For instance, which couplings have the properties that the corresponding c-Riemann solvers are $\mathbf{L}_{\text{loc}}^1$ -continuous with respect to the initial data? This property is satisfied by the Lax Riemann solver. Is it possible to characterize some invariant domains for Cauchy problems? This would be a first step toward the solution of the Cauchy problems in the large.

About coherence, we emphasize that its failure is not due to bad modeling, but reflects some physical phenomenon; this is the case, for instance, of the chattering of valves [19–22]. The issue of how to modify a valve to get coherence is tackled in [20]. The same problem obviously occurs for other mechanical devices, for instance, compressors.

Acknowledgements

M.D.R. thanks R. Borsche, M. Garavello, M. Gugat and M. Herty for valuable discussions. A.C. and M.D.R. acknowledge financial support from (a): the PRIN 2022 project *Modeling, Control and Games through Partial Differential Equations* (D53D23005620006), funded by the European Union - Next Generation EU; (b): the INdAM - GNAMPA Research Project *Modeling and Analysis through Conservation Laws*, code CUP E53C23001670001. A.C. acknowledges financial support from FAR and FIRB Research Projects of the University of Ferrara.

Section	Coupling	Two-way flow	Two pressures	Uniqueness	Coherence
4.1	$p(\rho_c^+) = p(\rho_c^-)$	YES	NO	YES	YES
4.2	$P(u_c^+) = P(u_c^-)$	YES	NO	NO	
4.2	$P(u_c^+) = P(u_c^-)$ and $F(u_c^+) \leq F(u_c^-)$	YES	NO	YES	YES
4.3	$\mathcal{E}(u_c^+) = \mathcal{E}(u_c^-)$	YES	NO	NO	
5.1	$v(u_c^+) \leq a_2$	NO	YES	YES	YES
5.2	$p_{a_2}(\rho_c^+) = p_{a_1}(\rho_c^-)$	NO	YES	YES	NO
6.1	$p(\rho_c^+) = \begin{cases} (1 + K_p^-)p(\rho_c^-) & \text{if } q_c^0 \leq 0 \\ (1 + K_p^+)p(\rho_c^-) & \text{if } q_c^0 > 0 \end{cases}$	YES	NO	NO	
6.1	$ q_c^0 \left((p(\rho_c^+)/p(\rho_c^-))^{\text{sign}(q_c^0)\kappa} - 1 \right) = K$	YES	NO	NO	
6.2	$p(\rho_c^+) = (1 + K_p^+)p(\rho_c^-)$	NO	NO	YES	YES
6.2	$q_c^0 \left((p(\rho_c^+)/p(\rho_c^-))^{\kappa} - 1 \right) = K$	NO	NO	YES	YES
7.1	several valves in [19–22]	YES/NO	NO	YES	YES/NO
7.2	$p(\rho_c^+) = p(\rho_c^-) - \Delta$	NO	NO	NO	
7.2	$p(\rho_c^+) = p(\rho_c^-) - \Delta$ and q -max	NO	NO	YES	NO
7.2	$q_c^0 = 0$ if $p(\rho_c^-) > p^{\text{set}} + \Delta$ $p(\rho_c^+) = \begin{cases} p^{\text{set}} & \text{if } p^{\text{set}} < p(\rho_c^-) \leq p^{\text{set}} + \Delta \\ p(\rho_c^-) & \text{if } p(\rho_c^-) \leq p^{\text{set}} \end{cases}$	NO	NO	YES	NO
8	$p_{a_2}(\rho_c^+) = p_{a_1}(\rho_c^-) - f_{\text{ext}}$	NO	YES	NO	
8	$p_{a_2}(\rho_c^+) = p_{a_1}(\rho_c^-) - f_{\text{ext}}$ and q -max	NO	YES	YES	NO
8	$p(\rho_c^+) = p(\rho_c^-) - \text{sign}(q_c^0) \Delta$	YES	NO	NO	
8	$p(\rho_c^+) = p(\rho_c^-) - \Delta$ and q -max	NO	NO	YES	NO
8	$p(\rho_c^+) = p(\rho_c^-) - K_p \frac{ q_c^0 q_c^0}{\rho_c}$	YES	NO	NO	
8	$p(\rho_c^+) = p(\rho_c^-) - K_p \frac{ q_c^0 q_c^0}{\rho_c}$ and q -max	NO	NO	YES	NO

Table 1: Overview of the coupling conditions and related results. Above, “ q -max” stands for “flow maximization”; “two pressures” refers to the possibility of having two different pressure laws, one in $x < 0$ and the other in $x > 0$.

References

- [1] M. K. Banda and M. Herty. Multiscale modeling for gas flow in pipe networks. *Math. Methods Appl. Sci.*, 31(8):915–936, 2008.
- [2] M. K. Banda, M. Herty, and A. Klar. Coupling conditions for gas networks governed by the isothermal Euler equations. *Netw. Heterog. Media*, 1(2):295–314, 2006.
- [3] M. K. Banda, M. Herty, and A. Klar. Gas flow in pipeline networks. *Netw. Heterog. Media*, 1(1):41–56, 2006.
- [4] R. Borsche and J. Kall. ADER schemes and high order coupling on networks of hyperbolic conservation laws. *J. Comput. Phys.*, 273:658–670, 2014.
- [5] R. Borsche and A. Klar. Kinetic layers and coupling conditions for macroscopic equations on networks I: The wave equation. *SIAM J. Sci. Comput.*, 40(3):A1784–A1808, 2018.
- [6] R. Borsche and A. Klar. Kinetic layers and coupling conditions for scalar equations on networks. *Nonlinearity*, 31(7):3512–3541, 2018.
- [7] A. Bressan. *Hyperbolic systems of conservation laws*, volume 20. Oxford University Press, Oxford, 2000.
- [8] A. Bressan, S. Čanić, M. Garavello, M. Herty, and B. Piccoli. Flows on networks: recent results and perspectives. *EMS Surv. Math. Sci.*, 1(1):47–111, 2014.
- [9] J. Brouwer, I. Gasser, and M. Herty. Gas pipeline models revisited: model hierarchies, nonisothermal models, and simulations of networks. *Multiscale Model. Simul.*, 9(2):601–623, 2011.
- [10] C. Buisson, J. Lesort, and J. Lebacque. Macroscopic modelling of traffic flow and assignment in mixed networks. In *Proc. 6th Int. Conf. on Computing in civil and building engineering*, volume 2. Berlin, 1995.

- [11] C. Chalons, P.-A. Raviart, and N. Seguin. The interface coupling of the gas dynamics equations. *Quart. Appl. Math.*, 66(4):659–705, 2008.
- [12] K. S. Chapman, P. Krishniswami, V. Wallentine, M. Abbaspour, R. Ranganathan, R. Addanki, J. Sengupta, and L. Chen. Virtual pipeline system testbed to optimize the us natural gas transmission pipeline system. Technical report, Kansas State Univ., Manhattan, KS (United States), 2005.
- [13] P. Colella. Glimm’s method for gas dynamics. *SIAM J. Sci. Statist. Comput.*, 3(1):76–110, 1982.
- [14] R. M. Colombo. Hyperbolic phase transitions in traffic flow. *SIAM J. Appl. Math.*, 63(2):708–721, 2002.
- [15] R. M. Colombo and M. Garavello. A well posed Riemann problem for the p -system at a junction. *Netw. Heterog. Media*, 1(3):495–511, 2006.
- [16] R. M. Colombo and M. Garavello. On the Cauchy problem for the p -system at a junction. *SIAM J. Math. Anal.*, 39(5):1456–1471, 2008.
- [17] R. M. Colombo, M. Herty, and V. Sachers. On 2×2 conservation laws at a junction. *SIAM J. Math. Anal.*, 40(2):605–622, 2008.
- [18] R. M. Colombo and F. Marcellini. Smooth and discontinuous junctions in the p -system and in the 3×3 Euler system. *Riv. Math. Univ. Parma (N.S.)*, 3(1):55–69, 2012.
- [19] A. Corli, M. Figiel, A. Futa, and M. D. Rosini. Coupling conditions for isothermal gas flow and applications to valves. *Nonlinear Anal. Real World Appl.*, 40:403–427, 2018.
- [20] A. Corli, U. Razafison, and M. D. Rosini. Coherence and flow-maximization of a one-way valve. *ESAIM Math. Model. Numer. Anal.*, 56(5):1715–1739, 2022.
- [21] A. Corli and M. D. Rosini. Coherence and chattering of a one-way valve. *ZAMM Z. Angew. Math. Mech.*, 99(6):e201800250, 25, 2019.
- [22] A. Corli and M. D. Rosini. Coherence of coupling Riemann solvers for gas flows through flux-maximizing valves. *SIAM J. Appl. Math.*, 79(6):2593–2614, 2019.
- [23] C. F. Daganzo. A finite difference approximation of the kinematic wave model of traffic flow. *Transportation Research Part B: Methodological*, 29(4):261–276, 1995.
- [24] M. Dick, M. Gugat, and G. Leugering. Classical solutions and feedback stabilization for the gas flow in a sequence of pipes. *Netw. Heterog. Media*, 5(4):691–709, 2010.
- [25] C. C. E. Division. *Flow of Fluids Through Valves, Fittings, and Pipe*. Technical paper. Crane Company, 1978.
- [26] F. Dubois and P. LeFloch. Boundary conditions for nonlinear hyperbolic systems of conservation laws. *J. Differential Equations*, 71(1):93–122, 1988.
- [27] S. A. Dyachenko, A. Zlotnik, A. O. Korotkevich, and M. Chertkov. Operator splitting method for simulation of dynamic flows in natural gas pipeline networks. *Phys. D*, 361:1–11, 2017.
- [28] H. Egger. A robust conservative mixed finite element method for isentropic compressible flow on pipe networks. *SIAM J. Sci. Comput.*, 40(1):A108–A129, 2018.
- [29] M. Garavello. A review of conservation laws on networks. *Netw. Heterog. Media*, 5(3):565–581, 2010.
- [30] M. Garavello and B. Piccoli. *Traffic flow on networks*. American Institute of Mathematical Sciences (AIMS), Springfield, MO, 2006.
- [31] M. Gugat and M. Dick. Time-delayed boundary feedback stabilization of the isothermal Euler equations with friction. *Math. Control Relat. Fields*, 1(4):469–491, 2011.
- [32] M. Gugat, M. Dick, and G. Leugering. Gas flow in fan-shaped networks: classical solutions and feedback stabilization. *SIAM J. Control Optim.*, 49(5):2101–2117, 2011.
- [33] M. Gugat and J. Giesselmann. Boundary feedback stabilization of a semilinear model for the flow in star-shaped gas networks. *ESAIM Control Optim. Calc. Var.*, 27:Paper No. 67, 24, 2021.
- [34] M. Gugat and M. Herty. Existence of classical solutions and feedback stabilization for the flow in gas networks. *ESAIM Control Optim. Calc. Var.*, 17(1):28–51, 2011.
- [35] M. Gugat, M. Herty, and S. Müller. Coupling conditions for the transition from supersonic to subsonic fluid states. *Netw. Heterog. Media*, 12(3):371–380, 2017.

- [36] M. Gugat, M. Herty, and V. Schleper. Flow control in gas networks: exact controllability to a given demand. *Math. Methods Appl. Sci.*, 34(7):745–757, 2011.
- [37] M. Gugat, G. Leugering, A. Martin, M. Schmidt, M. Sirvent, and D. Wintergerst. MIP-based instantaneous control of mixed-integer PDE-constrained gas transport problems. *Comput. Optim. Appl.*, 70(1):267–294, 2018.
- [38] M. Gugat, R. Schultz, and M. Schuster. Convexity and starshapedness of feasible sets in stationary flow networks. *Netw. Heterog. Media*, 15(2):171–195, 2020.
- [39] M. Gugat and S. Ulbrich. Lipschitz solutions of initial boundary value problems for balance laws. *Math. Models Methods Appl. Sci.*, 28(5):921–951, 2018.
- [40] M. Herty. Modeling, simulation and optimization of gas networks with compressors. *Netw. Heterog. Media*, 2(1):81–97, 2007.
- [41] M. Herty, J. Mohring, and V. Sachers. A new model for gas flow in pipe networks. *Math. Methods Appl. Sci.*, 33(7):845–855, 2010.
- [42] Y. Holle. Kinetic relaxation to entropy based coupling conditions for isentropic flow on networks. *J. Differential Equations*, 269(2):1192–1225, 2020.
- [43] Y. Holle, M. Herty, and M. Westdickenberg. New coupling conditions for isentropic flow on networks. *Netw. Heterog. Media*, 15(4):605–631, 2020.
- [44] S. Hossbach, M. Lemke, and J. Reiss. Finite-difference-based simulation and adjoint optimization of gas networks. *Math. Methods Appl. Sci.*, 45(7):4035–4055, 2022.
- [45] R. J. LeVeque. *Numerical methods for conservation laws*. Birkhäuser Verlag, Basel, 1990.
- [46] Y. Mantri, M. Herty, and S. Noelle. Well-balanced scheme for gas-flow in pipeline networks. *Netw. Heterog. Media*, 14(4):659–676, 2019.
- [47] Y. Mantri and S. Noelle. Well-balanced discontinuous Galerkin scheme for 2×2 hyperbolic balance law. *J. Comput. Phys.*, 429:Paper No. 110011, 13, 2021.
- [48] D. Modesti and S. Pirozzoli. Direct numerical simulation of supersonic pipe flow at moderate Reynolds number. *Int. J. Heat Fluid Flow*, 76:100–112, 2019.
- [49] A. Morin and G. A. Reigstad. Pipe networks: Coupling constants in a junction for the isentropic euler equations. *Energy Procedia*, 64:140–149, 2015.
- [50] G. A. Reigstad. Existence and uniqueness of solutions to the generalized Riemann problem for isentropic flow. *SIAM J. Appl. Math.*, 75(2):679–702, 2015.
- [51] G. A. Reigstad, T. Flåtten, N. Erland Haugen, and T. Ytrehus. Coupling constants and the generalized Riemann problem for isothermal junction flow. *J. Hyperbolic Differ. Equ.*, 12(1):37–59, 2015.
- [52] D. Rose, M. Schmidt, M. C. Steinbach, and B. M. Willert. Computational optimization of gas compressor stations: MINLP models versus continuous reformulations. *Math. Methods Oper. Res.*, 83(3):409–444, 2016.
- [53] M. Schmidt, M. C. Steinbach, and B. M. Willert. High detail stationary optimization models for gas networks. *Optim. Eng.*, 16(1):131–164, 2015.
- [54] E. F. Toro. *Riemann solvers and numerical methods for fluid dynamics*. Springer-Verlag, Berlin, 1997. A practical introduction.